HYDRODYNAMIC STUDIES OF COARSE, FINE AND NANO PARTICLES IN A CYLINDRICAL FLUIDIZED/ SPOUTED BED: CFD SIMULATION

A Thesis Submitted to the

National Institute of Technology, Rourkela

In Partial Fulfillment for the Requirements

Of

Master of Technology (R) Degree

In

CHEMICAL ENGINEERING

By

Ms. Pranati Sahoo

Roll No. 609CH308

Under the guidance of

Dr. (Mrs.) Abanti Sahoo

Department of Chemical Engineering
National Institute of Technology
Rourkela-769008

National Institute of Technology
Rourkela

CERTIFICATE

This is to certify that M.Tech. (Res.) thesis entitled, "**Hydrodynamic Studies of Coarse, Fine and Nano Particles in a Cylindrical Fluidized / Spouted Bed: CFD Simulation**" submitted by **Ms. Pranati Sahoo** in partial fulfillments for the requirements of the award of Master of Technology (R) degree in Chemical Engineering at National Institute of Technology, Rourkela is an authentic work carried out by her under my supervision and guidance. She has fulfilled all the prescribed requirements and the thesis, which is based on candidate's own work, has not been submitted elsewhere.

Supervisor
Dr. (Mrs.) Abanti Sahoo
Department of Chemical Engineering,
National Institute of Technology,
Rourkela - 769008,
Orissa

ACKNOWLEDGEMENT

CONTENTS

LIST OF TABLES

LIST OF FIGURES

ABSTRACT

The fluidization characteristics or hydrodynamic behaviours of coarse (regular / irregular), fine and nano particles have been studied in a fluidized and/or spouted bed for gas-solid system. A stirrer and external force (equivalent centrifugal force) have been used with fine and nano particles respectively for smooth fluidization. The speed of rotation of stirrer with fine particles and frequency of application of external force (magnitude of force) with nano particles were also varied for analyzing the fluidization characteristics. Experiments were carried out in a cylindrical column by varying different system parameters (viz. static bed height, particle size, particle density and superficial velocity of the medium, speed of rotation of stirrer and spout diameter). Fluidization characteristics, such as bed expansion ratio, bed fluctuation ratio, bed pressure drop, minimum fluidizing/spouting velocity and fluidization index of coarse (regular / irregular), fine and nano particleshave been tried to be analyzed by developing correlations on the basis of dimensional less analysis. Finally calculated values of different fluidization characteristics have been compared against the experimentally observed values. The comparison results show a good agreement among the experimental and calculated values thereby indicating the application of these developed correlations over a wide range of parameters.

CFD simulation has also been carried out for the hydrodynamic behaviours. Finally calculated values of these fluidization characteristics obtained through CFD simulation have been compared against the experimentally observed values. The results show a good agreement thereby implying the design of fluidizer for gas-solid systems can be optimum design for many chemical industries. The technique of external force application can also be suitably used in industries for handling nano particles with increased efficiencies.

Key words: - Fluidized bed, Spouted bed, Coarse / Fine / Nano particles, hydrodynamic studies, Dimensionless analysis and CFD simulation

CHAPTER – 1

INTRODUCTION

INTRODUCTION

1.1 Fluidization

Fluidization is one of the best ways of interacting solid particles with fluid when drag force is acting on the solid particles is equal to gravity force / weight of the particles. The variables affecting the quality of fluidization i.e. Fluid flow rate, Fluid inlet, Particle size, Fluid densities, Static bed height. That is why the present work aims to study the effect of different parameters on hydrodynamic behaviors of fluidized / spouted bed.

1.2 Need for CFD

Computational Fluid Dynamics (CFD) is a whole new field which needs to be explored well. Over the recent years there have been various computational works but in comparison to the huge experimental data available, more works in the field of CFD is required. CFD predictions can be verified with the experimental data and results and can be checked if they hold good or not. With the experimental work being tedious, CFD helps in predicting the fluid flow, behavior of the fluidized bed and various hydrodynamic characteristics. CFD actually helps in modeling the prototype of a process and through CFD predictions one can apply those parameters to achieve the desired results. Thus the complex hydrodynamics of fluidization could be understood using CFD.

1.3 Advantages of Fluidization

There are several advantages of fluidized bed relative to fixed bed processes such as; ability to maintain uniform temperature gradients, significantly lower pressure drops which reduces low pumping costs, catalysts can be continuously added / withdrawn / reactivated due to

low inter particle diffusion resistance and low gas - solid and liquid – solid mass transfer resistance . Bed channeling / plugging minimized due to vigorous movement of solid particles in fluidized bed. High reactant conversion i.e. completely mixed flow pattern in reaction kinetics achieved in fluidized bed by low investment for specification of feed and product and ability to operate reactor in a continuous state by uniform solid particle mixing in fluidized bed.

1.4 Application of Fluidization

It has extensive industrial applications due to above mentioned advantages of the fluidized bed, in nuclear power plants, chemical, biochemical and metallurgy industry. It is extensively used in Petroleum industry for fluid bed catalytic cracking. In chemical operation i.e. gasification and carbonization of coal, roasting of sulphur ores, reduction of iron oxides, blending of granular materials, granulation of fertilizer, combustion, incineration, and pyrolysis of shale and in physical operation i.e. drying of solids such as crushed minerals, sand, polymers, pharmaceuticals, fertilizers and crystalline products, coating of metals with plastic and particles in pharmaceutical and agricultural industries, transportation, granulation of solids, heating, cooling and water and waste treatment etc. it is used. The commercial applications of fluidization are fluid catalytic cracking, reforming, Fischer- Tropsch synthesis, catalyst regeneration, granulation (growing particles), oxidation reactions involving solid catalyzed gas phase reactions, fluid coking, bio-oxidation process for waste water treatment, transportation of solids like slurry pipeline for coal.

1.5 Objective of the work

The aim of the present work could be summarized as follows

- ❖ To study the fluidization characteristics of different sized solid particles (5mm to 70nm) in both fluidized bed as well as spouted bed.

- ❖ Effect of different system parameters on hydrodynamic behaviors of the bed in a cylindrical fluidized bed.

- ❖ Correlate the different bed dynamics of coarse regular/ irregular and fine particles by varying system parameters in both fluidized bed and spouted bed.

- ❖ CFD Simulation for the bed expansion of fine Particles for prediction of its characteristics.

- ❖ Validation of bed characteristics of fine alumina powder with experimental and CFD simulation.

1.6 Thesis Layout

The second chapter gives a comprehensive review of literature related to the hydrodynamic characteristics in a fluidized bed as well as spouted bed. It includes the computational aspect as well as the hydrodynamics behaviors of gas-solid fluidization by CFD methodologies. The third chapter deals with the experimentation of different size materials. The fourth chapter deals with comparison of hydrodynamics behaviors of different particle sizes in a gas – solid bed. Chapter five deals with the result part obtained from simulations which have been discussed thoroughly. The correlations for bed dynamics of different particle sizes in gas – solid bed have been discussed by varying system parameters in chapter six as results and discussion. In chapter seven conclusions have been drawn on present work and scope of the future work has also been discussed.

CHAPTER – 2

LITERATURE SURVEY

LITERATURE SURVEY

The fluidized bed is one of the best known contacting methods used in processing industries. The solid particles are transformed to fluid – like state through the contact with fluid i.e. gas or liquid or both which is allowed to pass through a distributor plate. Under the fluidized state, the gravitational force pull on solid particles is offset by the fluid drag force on them, thus the particles remain in a semi – suspended condition. At the critical value of fluid velocity, the upward drag force exerted by solid particles become exactly equal to the downward gravitational force, causing the solid particles to be suspended within the fluid. At this critical value, the bed is said to be fluidized and exhibits behaviors of fluid.

2.1 Types of Fluidized Bed

According to flow regime the fluidized bed is divided into following types (**Fig. – 2.1**)

- Fixed bed
- Incipiently fluidized bed
- Smooth fluidized bed
- Bubbling fluidized bed
- Turbulent fluidized bed
- Channeling fluidized bed
- Slugging fluidized bed
- Spouted bed

2.2 Fluidized Bed versus Spouted Bed

The difference between fluidized bed and spouted bed lies in the dynamic behaviors of the solid particles. Such as -

- In a fluidized bed, air is passed through a uniform distributor / multi orifice plate to float the particles which move up and down. Spouted beds are gas – particle contactor in

which the gas is introduced through a single orifice at the center of a conical or flat base, instead of a multi orifice, resulting in a systematic cyclic pattern of solid movement inside the bed.

- The fluidized bed is used to describe the condition of fully suspended particles in a fluid stream whereas spout bed apparatus used in those areas where intense contact of fluid – solid systems is required and to determine the effectiveness of fluid – solid contact.

- A fluidized bed consists of two phases: the bubble phase and the emulsion phase (**Kunii and Levenspiel, 1991**). In bubble phase, the bubbles are present in the core region of the bed and the emulsion phase is only occupied near wall region of the bed. The bubble phase slowly increases linearly and the emulsion phase decreases with increasing the fluidizing velocity and reaches a constant minimum value of fluidization velocity (**Fig.- 2.2**).

A spouted bed has three different regions each with its own specific flow behaviors: the annulus, the spout and the fountain (**Mathur and Epstein, 1974**). At stable spouting process, a spout appears in the center, a fountain above the bed surface and an annulus between the spout and the wall.

- The spout and the fountain are similar to fluidized beds with particles dynamically suspended, while the annulus region is more like a packed bed or moving bed. At partial spouting, there are only two distinct regions, an internal spout that is similar to a fluidized bed and the surrounding packed particle region which is similar to a packed bed.

- The advantages of spouted beds over the conventional fluidized bed are its ability to process coarse, sticky and heat sensitive materials.

- The spouting and its stability, operating condition, spouting bed height along with the changing phenomenon from spouting to bubbling, slugging etc. depends on many factors like particle size, orifice size of spouting, flow rate of fluidizing fluid, bed height and the density of particles used. For a given solid material contacted by a specific fluid in a vessel of fixed geometry, there exists a maximum spoutable bed depth, beyond which the spouting action does not exists but it is replaced by a poor quality fluidization. The minimum spouting velocity at this bed depth can be 1.25 to 1.5 times the corresponding minimum fluidization velocity, U_{mf}.

2.3 Geldart's Classification of Particles

The Geldart's classification system is used to identify and distinguish between the fluidization properties of particulate materials in a vertical gas-solid fluidized bed at given conditions (**Kunii and Levenspiel, 1991**). In this system, gas flows upward through a distributor with a velocity which is enough to fluidize the particle but this velocity is not so much that particle can go out of the column. According to this system, particles which show similar kind of fluidization behavior are classified into the same group which is based on particle diameter and density difference of two phases.

In 1973, Professor D. Geldart proposed the grouping of powders in to four so-called "Geldart Groups" as follows.

Group A Particles: Such particles are having size between 20 and 100 μm, and the particle density less than 1.4 g/cm^3.

Group B Particles: These particles lie between 40 and 500 μm size and the particle density between 1.4 to 4 g/cm^3 and exhibit incipient fluidization.

Group C Particles: This group contains extremely fine and consequently the most cohesive particles. With a size of 20 to 30 μm, these particles fluidize under very difficult to achieve conditions, and may require the application of an external force, such as mechanical agitation, magnetic field, electric field, and centrifugal field etc.

Group D Particles: The particles in this region are above 600 μm and typically have high particle densities. Fluidization of this group requires very high fluid energies and is typically associated with high levels of abrasion. Drying grains and peas, roasting coffee beans, gasifying coals, and some roasting metal ores are such solids, and they are usually processed in shallow beds or in the spouting mode.

Fluidization quality is closely related to particle intrinsic properties such as particle size, particle density, size distribution of particle and its surface characteristics. As the particle size decreases the cohesive force (i.e. Vander Wall Force) for the particle increases. As a result of this the fluidization of cohesive materials for fine particle becomes much more difficult in comparison to the larger size particle. The fine particle in Group C (small particle size and low particle density) fluidize poorly in Geldart's classification chart due to their strong inter-particle cohesive forces, exhibiting problems like channeling, resulting in no fluidization of particles and also tend to rise as a slug of solids. Group C particles are cohesive in nature (Geldart1973),

are unsuitable for fluidization because they tend to form agglomerates since they are having strong inter particle forces between them. Nano sized powders, fall under the Geldart group C (< 30 microns) classification, which means that fluidization is expected to be difficult due to cohesive forces i.e. strong inter particle forces. Nano size particles differ from conventional Geldart C particles not only in being much smaller size but also in having a very low bulk density which has also been pointed out by Geldart in his classification map. Therefore, development of the reliable technique to improve the fluidization quality of cohesive fine powders is essential.

2.4 Improvement of Fluidization Quality

The fluidization quality of fine / nano particles has been tried to be improved by following two techniques:-

(I)   By external force   (II)   By altering the intrinsic properties of particles

The external force means using vibration, sound amplifier, magnetic field, electric field, centrifugal field and mechanical agitation for improving the bed fluidity or flow ability of fine cohesive powders.

The other one done by modifying surface characteristics by mixing with other particles having different size or shape because of higher gravity force.

2.5 Parameters Studied

The parameters studied during a fluidization/spouting process are

- Minimum Fluidization(U_{mf}) / Spouting Velocity (U_{ms})

- Bed Pressure Drop (Δp)
- Bed Expansion Ratio (R)

- Bed Fluctuation Ratio (r)
- Fluidization Index (FI)

2.5.1 Minimum Fluidization Velocity:

When a fluid passes upwards through the interstices of a bed of solids without the slightest disturbance of the solids, the bed is called a fixed bed. With further increase in the velocity of fluid, the entire bed of solids is suspended and its weight is counterbalanced by the buoyancy force. At this point, the bed of solids starts behaving like a fluid. This is called onset of fluidization and the velocity of fluid at which it happens is known as the minimum fluidization / spouting velocity, which is one of the most important parameter for the design of fluidizers.

Cardoso et al. (2008) calculated minimum fluidization velocity of fine particle and **Padhi et al. (2009)** presented hydrodynamic properties i.e. minimum fluidization velocity, bed pressure drop, minimum bubbling velocity, minimum slugging velocity, bubbling velocity, expansion ratio, fluctuation ratio of gas solid fluidization in a hexagonal bed.

2.5.2 Pressure drop:

The pressure drop through the bed is another important parameter which controls the channel and slug formation and thereby mixing of the bed material with the fluidizing fluid.

In fluidization process **(Kunii and Levenspiel, 1991),** at low flow rates of fluid the bed behaves like a packed bed, where the pressure drop is approximately proportional to gas velocity without any change in the bed height. With further increase in velocity, the bed materials start moving and the fluidization begins. Once the bed is fluidized, the pressure drop across the bed remains constant, but bed height continues to increase with increasing flow of fluid.

In spouting process **(Mathur and Epstein, 1974),** the bed pressure drop gradually increases with increase in velocity up to certain limit and then decreases up to certain point after which it remains constant.

Zhiping et al. (2007) investigated the minimum fluidization velocities of quartz, sand and glass beads under different pressures of 0.5, 1.0, 1.5 and 2.0 MPa. They concluded that the minimum fluidization velocity decreases with the increasing of pressure and the minimum fluidization velocities is stronger for larger particles than for smaller ones by the influence of pressure.

2.5.3 Bed Expansion Ratio:

Bed Expansion Ratio is used to describe the characteristics of bed height during fluidization condition. This is quantitatively defined as the ratio of average expanded bed height of a fluidized/spouted bed to the initial static bed height at a particular flow rate of the fluidizing medium (above the minimum fluidizing velocity). Average expanded bed height is the arithmetic mean of highest and lowest level occupied by top of the fluidized bed. It is denoted by "R".

$$\mathbf{R} = \left(\frac{H_{avg}}{H_{static}}\right) = \left(\frac{H_{max}+H_{min}}{2*Hs}\right) \qquad (2.1)$$

This term used in the spouted bed is also having the same meaning at fluidization condition. It is an important parameter for fixing the height of fluidized bed required for a particular service. The expansion ratio of a fluidized bed depends on excess gas velocity above the minimum fluidization, particle size (d_p), and initial bed height (H_s).

Sau et al. (2010) studied the expansion behaviors of tapered fluidized bed systems by specifying the height of the bed. The expanded heights of tapered fluidized beds and bed expansion ratio for spherical and non-spherical particles have been calculated by them. Based on dimensional analysis, models have been developed as a function of geometry of tapered bed, static bed height, particle size, density of solid and gas and superficial velocity of the fluidizing medium.

2.5.4 Bed Fluctuation Ratio:

The term bed fluctuation ratio is used to describe the characteristics of the bed during fluidization/spouting process. This is quantitatively defined as the ratio of the highest and lowest levels which the top of the bed occupies at any particular fluid flow rate. It is denoted by "r".

$$\mathbf{r} = \left(\frac{\mathbf{H_{max}}}{\mathbf{H_{min}}}\right) \tag{2.2}$$

Bed fluctuation ratio has widely been used of quantify fluidization quality. A lower value of fluctuation ratio is indicative of improved fluidization quality with less fluctuation of the top surface of the bed in fluidized condition. [**Singh et al. (2006), Sahoo, A. (2010) and Kumar et al. (2007)**] explained bed expansion and fluctuation in cylindrical fluidized beds for irregular particles of binary mixtures in a gas-solid system using stirred promoters where effects of different system parameters have been analyzed.

2.5.5 Fluidization Index:

Fluidization index is the ratio of pressure drop across the bed to the weight force exerted by the bed material per unit area of cross-section of the column. For ideal fluidization, fluidization index is 1.

$$\mathbf{F. I.} = \left[\frac{\Delta P}{(W/A)} \right] \qquad (2.3)$$

Fluidization index (**Singh et.al 2005**) which gives a measure of the degree of uniform expanded bed during fluidization condition. The higher the ratio, the bed can hold more gas between the minimum fluidization and bubbling point.

2.6 Previous Works

2.6.1 Spouting Process:

Olazar et al. (1993) studied binary mixtures of glass spheres of particle size between 1 and 8 mm, in stable regime and without segregation, in a conical spouted bed. The effects of the stagnant bed height, the mixture composition and the gas velocity on bed stability and bed segregation have been analyzed. **Rooney et al. (1974)** studied hydrodynamic behaviors of spouted beds of sand particles and found the range of particle sizes that can be spouted extends downwards to atleast 90 - 150 µm. They also investigated further whether a bed of particles of given size can be maintained in the spouting condition or, not. It was concluded that particle size strongly dependent on the diameter of the inlet orifice.

Shan et al. (2001) explained fixed bed regime and spouting bed regime by carried out experiments successively with the increase in superficial gas velocity for Geldart - A and D

particles in a conical bed using three cone angles. The characteristics of the regime for Geldart-A powder differs from that for the Geldart-D particles due to the disappearance of partially fluidized bed regime.

Olazar et al. (1994) studied the hydrodynamic behavior of a nearly flat base spouted bed (angle 150^0) in a pilot plant unit, using solids of different densities and particle sizes and with different values of the contactor inlet diameters. It was observed that the equation of Mathur and Gishler with an exponent of 0.10 for the (D_o/D_c) modulus is suitable for calculation of the minimum spouting velocity. Original correlations for prediction of the maximum pressure drop for stable operation and bed voidage in the bed expansion are also proposed.

Zhong et al. (2006) experimentally studied the maximum spoutable bed height for a spout-fluid bed (cross-section of 0.3 m × 0.03 m and height of 2 m) packed with Geldart group D particles. The effects of particle size, spout nozzle size and fluidizing gas flow rate on the maximum spoutable bed height has been studied. It was observed that the maximum spoutable bed height of spout-fluid bed decreases with increasing particle size and spout nozzle size. The increase in fluidizing gas flow rate leads to a sharp decrease in the maximum spoutable bed height.

Bacelos et al. (2008) carried out experimental investigation to evaluate the stable spouting regime in conical spouted beds using four particle mixtures: a reference (mono particles), a binary mixture, and two ternary mixtures with flat and Gaussian distributions respectively using a high-viscosity Newtonian fluid, glycerol. The mixtures were selected for particle sizes (d_p) ranging from 1.09 to 4.98 mm and particle size ratios ranging from 1.98 to 4.0. Experimental data show the pressure fluctuation signals of the bed for stable spouting. However, the analysis of skewness of curves of pressure fluctuation as a function of air velocity appears not sufficient

to identify a particular flow regime. For glycerol in the spouting regime, the standard deviation was noted to increase with increasing glycerol concentration due to the growth of inter particle forces. They have also discussed the implications of these research findings on the drying of suspensions in conical spouted beds using glass bead mixtures.

Olazar et al. (1994) have proved that conical spouted beds allow for stable operation with sawdust and with wood residues, even with mixtures of these materials of wide particle size range and without being diluted with an inert solid. Peculiar hydrodynamic characteristics have been observed with sawdust. From the hydrodynamic study of sawdust, the ranges of the contactor geometric factors (cone angle, inlet diameter/base diameter ratio, inlet diameter/particle diameter ratio) for which operation is stable have been determined.

2.6.2 Fine Particle Fluidization:

Wang et al. (1997) carried out experiments on the fluidization using fine particles (Geldart group C) with mean sizes 0.01-18.1 μm and densities 101~8600 kg/m^3. Experimental results show that the fine particles fluidization process usually involves plugging, channeling, disrupting, and agglomerating. When fluidized, the entities fluidized generally consist of particle agglomerates varying in size from the largest at the bottom of the bed (some even defluidized) to the smallest at the top (some even unassociated to discrete particles). Best to fluidize are the agglomerates which have reached a uniform equilibrium size after repeated solids circulation. Lowering agglomerate density proves to be an effective measure for improving the fluidization quality of fine particles.

Laszuk et al. (2008) explained uniform fluidization of a group-C material (particle size ≤ 50 μm). An experimental plant in which the hydraulic resistance of the bed was measured as a function of its height and the rotational speed of the mixer during the fluidization is described. It is established that an increase in the height of the stationary bed above 0.01m leads to an increase in hydraulic resistance on transition to the fluidized state, especially at low rotational speeds of the mixer.

Kusakabe et al. (1989) fluidized fine particles including some submicron powders are fluidized under reduced pressures and the minimum fluidization velocity was determined in a shallow bed. When the gas throughput is not enough in a deep bed, only an upper part of the bed is fluidized and the rest is quiescent.

Avidan et al. (1982) investigated bed expansion of fine powders with two high aspect ratio fluid beds i.e. expanded top bed and a circulating system. **Xu et al (2006)** investigated the effects of vibration on fluidization of fine particles (4.8 – 216 μm size in average) and concluded that the fluidization quality is enhanced under mechanical vibration leading to larger bed pressure drops at low superficial gas velocities U_{mf}. The effectiveness of vibration on improving fluidization is strongly dependent on the properties (Geldart particle type, size-distribution and shape) of the primary particles used and the vibration parameters (frequency, amplitude and angle) applied. The possible roles of mechanical vibration in fine particle fluidization have been studied with respect to bed voidage, pressure drop, agglomeration, and tensile strength of bed particle. Vibration is found to significantly reduce both the average size and the segregation of agglomerates in the bed thus improving the fluidization quality of cohesive particles. Also, vibration can dramatically reduce the tensile strength of the bed particle. Obviously, vibration is

an effective means to overcome the inter particle forces of fine powders in fluidization and enhance their fluidization quality.

Mawatari et al. (2005) studied to clarify the operational ranges for vibro-fluidization of fine cohesive particles (glass beads, d_p = 6 micron) by decreasing and increasing gas velocity. In the increasing gas velocity method, a cross-point was obtained from the relationship between the gas velocity and the bed pressure drop. At one of the gas velocities at these cross-points, the bed void fraction reached its maximum. **Jaraiz et al. (1992)** estimated the inter particle cohesive forces from pressure drop versus bed expansion data for packed vibrated beds of very fine particles subjected to a gentle up flow of gas. A consequence of this analysis is a prediction of the Geldart C/A transition.

Russo et al. (1995) studied non fluent catalyst particles of 0.5 - 45 μm by carried out sound assisted fluidization in a 145 mm i.d. column. Different amounts of solids were fluidized in the column with a loudspeaker generated an acoustic field, above the bed, with a sound pressure level (referred to 20 μPa) varying from 110-140 dB and a frequency varying from 30 to 1000 Hz.

Valverde et al. (2009) investigated the behavior of a fluidized bed of fine magnetite particles, a naturally cohesive powder which is affected by a cross flow magnetic field. It was observed that the fluidized bed displays a range of stable fluidization even in the absence of an external magnetic field. Upon application of the magnetic field, the interval of stable fluidization is extended to higher gas velocities and bed expansion is enhanced.

2.6.3 Nano Particle Fluidization:

Jung et al. (2002) carried out experiments on fluidization and collapsing bed with 'Tullanox', 10 nm dia. fumed silica. The minimum fluidization velocity was determined to be 0.0115 m/s at the unusually low volume fraction of solids of 0.0077. The solids volume fraction was measured using a γ -ray densitometer. Fluidization was without large bubbles, with a high bed expansion ratio. The highest granular temperature was of the order of that of Geldart B particles, as measured by **Cody et al. (1996).**

Zhu et al. (2005) experimentally studied the effect of different parameters on the fluidization characteristics of nano particle agglomerates. Taking advantage of the extremely high porosity of the bed, optical techniques were used to visualize the flow behavior, as well as to measure the sizes of the fluidized nano particle agglomerates at the bed surface. Upon fluidizing 11 different nano particle materials, two types of fluidization behavior systematically were investigated for nano particle, agglomerate particulate fluidization (APF) and agglomerate bubbling fluidization (ABF). Using the Ergun equation, the pressure drop was measured and bed height, average agglomerate size and voidage at minimum fluidization were predicted by the model. The minimum fluidization velocities for APF nano particles were calculated.

Huang et al. (2008) investigated the nano-particles mixing behavior in a nano-agglomerate fluidized bed (NAFB) using R972, a kind of nano-SiO_2 powder, by the nano particle coated phosphors tracer method. The axial and radial dispersion coefficients were calculated and observed that the axial solids dispersion coefficient increased with increasing superficial gas velocities, and ranged between 9.1×10^{-4} and 2.6×10^{-3} m^2/s. There was a step increase in the axial solids dispersion coefficient between the particulate, bubbling and turbulent fluidization

regimes. As the superficial gas velocity increased, the radial solids dispersion coefficient increased gradually, from 1.2×10^{-4} to 4.5×10^{-4} m^2/s. Authors have concluded that the density difference between the fluidized particles and fluidizing medium, kinetic viscosity of the fluidizing medium, and other hydrodynamic factors like superficial velocity of the fluidizing medium and average diameters of the fluidized particles, were the key factors in the solids mixing in the fluidized beds.

Hakim et al. (2005) studied the fluidization behavior of fumed silica, zirconia, and iron oxide nano powders at atmospheric and reduced pressures. The characteristics of fluidized aggregates of nano particles were studied by using a high speed laser imaging system and the effect of different particle interactions (London vander Waals, liquid bridging and electrostatic) at atmospheric pressure. The reduction of inter particle forces resulted in a reduced aggregate size and minimum fluidization velocity (U_{mf}) and an increased bed expansion. Nano particles were also fluidized at reduced pressure (16 Pa) with vibration to study the effect of low pressure on the minimum fluidization velocity.

Nam et al. (2004) fluidized 12-nm silica particles by coupling aeration with vibration with frequency in the range of 30 to 200 Hz, and vibrational acceleration in the range of 0 to 5 m/s^2. The minimum fluidization velocity was approximately 0.3 – 0.4 cm/s, and essentially independent of the vibrational acceleration. However, the bed expanded almost immediately after the air was turned on, reaching bed expansion of three times the initial bed height or higher. Thus the bed appeared to exhibit a fluid like behavior at velocities much lower than the minimum fluidization velocity. Fluidization of nano particles was achieved as a result of the formation of stable, relatively large, and very porous agglomerates. Practically no bubbles or

elutriation of particles was observed. **Wang et al. (2007)** explained the behavior of gas-particle interaction in a fluidized bed which depends strongly on the size of the particles being fluidized. Fluidization characteristics of macro-sized particles, from several tens of microns to several millimeters, are well described by the Geldart [1973] classification. Degussa Aerosil R974 powder, with a primary particle size of 12 nm, was fluidized using nitrogen in a cylindrical vessel of 50 mm i.d. and 900 mm height. Characteristics of incipient fluidization are analyzed in relation to variations in the initial packed bed conditions. Bed collapse experiments were performed and the results are used for assessing fluidization characteristics of the particles. It was found that nano sized particles possess characteristics of both Group A and Group C of Geldart classification.

2.6.4 CFD Simulation:

Computational Fluid dynamics (CFD) is a powerful tool to predict the fluid mechanics that uses numerical methods and algorithms to solve and analyze problems that involve fluid flows and also describing the proper design of such system. CFD simulation method widely used to analyze the fluid flow behaviors as well as heat and mass transfer process and chemical reaction.

It has been widely used in an attempt to model gas- solid fluidized beds using two different approaches / methods: a discrete method (Lagrangian model) and a continuous method (multi fluid or Eulerian – Eulerian model). In discrete method, the fluid phase is described by Navier- stoke equation with the use of inter phase forces of two phases, in this case, the gas is treated as the continuous phase and the solid as the discrete phase. In Eulerian model, the different phases are treated as interpenetrating continua by incorporating the concept of phase

volume fraction and to solve the conservation equation for each phase. That is why in case of fluidization, the two phases are treated as interpenetrating continua where the solids are treated as discrete, and the particle trajectory is obtained by solving the Newton's equation of motion. The finite volume method is used for solving or discretized the governing equations i.e. conservation of mass, momentum, energy.

2.6.4.1 Advantages of CFD:

Major advancements in the area of gas-solid multiphase flow modeling offer substantial process improvements that have the potential to significantly improve process plant operations. Prediction of gas solid flow fields, in processes such as pneumatic transport lines, risers, fluidized bed reactors, hoppers and precipitators are crucial to the operation of most process plants. In recent years, computational fluid dynamics (CFD) software developers have focused on this area to develop new modeling methods that can simulate gas-solid flows to a much higher level of reliability. As a result, process industry engineers are beginning to utilize these methods to make major improvements by evaluating alternatives.

The key advantages of CFD are:

1. It provides the flexibility to change design parameters without the expense of hardware changes. Hence it costs less than laboratory or field experiments, allowing engineers to try more alternative designs than would be feasible otherwise.

2. It has a faster turnaround time than experiments.

3. It guides the engineer to the root of problems, and is therefore well suited for trouble-shooting.

4. It provides comprehensive information about a flow field, especially in regions where measurements are either difficult or impossible to obtain.

2.6.4.2 Computational Model

In the present work, an Eulerian granular multiphase model is adopted where gas and solid phases are all treated as continua interpenetrating and interacting with each other everywhere in the computational domain. The pressure field is assumed to be shared by all the two phases, in proportion to their volume fraction. The motion of each phase is governed by respective mass and momentum conservation equations.

Continuity equation:

$$\frac{\partial}{\partial t}(\varepsilon_k \rho_k) + \nabla(\varepsilon_k \rho_k u_k) = 0 \tag{2.4}$$

The volume fraction of the two phases satisfies; $\varepsilon_g + \varepsilon_s = 1$ (2.5)

Momentum equations:

For gas phases

$$\frac{\partial}{\partial t}(\rho_g \varepsilon_g u_g) + \nabla(\rho_g \varepsilon_g u_g u_g) = -\varepsilon_g \nabla p + \nabla \tau_g + \rho_g \varepsilon_g g + F_{i,g} \tag{2.6}$$

For solid phase

$$\frac{\partial}{\partial t}(\rho_s \varepsilon_s u_s) + \nabla(\rho_s \varepsilon_s u_s u_s) = -\varepsilon_s \nabla p - \nabla p_s + \nabla \tau_s + \rho_s \varepsilon_s g + F_{i,s} \tag{2.7}$$

Where L.H.S. represents the temporal and spatial transport term and R.H.S. represents various interacting forces. The first term in R.H.S. of eq^n (2.6) and (2.7) is represents the hydrodynamic pressure of solid and gas phases. The second term i.e. τ_g and τ_s in the R.H.S of eq^n (2.6) and third term of eq^n (2.7) represents stress-strain tensors of gas and solid phase respectively. The second term in the R.H.S of eq^n (2.7) represents additional solid pressure due to solid collisions. The terms $F_{i,g}$ and $F_{i,s}$ of the above momentum equations represent the inter-phase momentum exchange respectively.

Inter-Phase Momentum Exchange:

Inter - phase momentum exchange F_i is the combination of different interaction forces i.e. lift force, drag force and added mass force between two phases i. e solid phase and liquid phase. It is represented as

$$F_i = F_L + F_D + F_{VM} \tag{2.8}$$

The lift force (F_L) does not used in 2D simulation because difficult to understand the complex mechanism of lift force in gas phase. The added mass force (F_{VM}) is not used in 2D simulation because added mass force is used when high frequency fluctuations of the slip velocity used. This force is much smaller than drag force when bubble fluidization or bubbly flow used. Thus only drag force (F_D) is used as inter – phase momentum exchange in 2D CFD simulation.

Gas – solid inter phase drag force:

The momentum exchange between two dispersed phases i.e. gas phase and solid phase has been considered for CFD simulation. The drag force is acting on a particles in gas – solid phase, is

represented by the product of momentum exchange coefficient and slip velocity between two phases. Gas – solid inter phase drag force is represented as

$$F_{D,gs} = K_{gs}(u_g - u_s)$$ (2.9)

Where K_{gs} is the inter phase exchange coefficient of gas – solid phase. It is calculated from Gidaspow drag model i.e. it is the combination of Ergun equation and Wen and Yu model.

When $\varepsilon_g \leq 0.8$

$$K_{gs} = 150 \frac{\varepsilon_s(1-\varepsilon_g)\mu_g}{\varepsilon_g d_p^2} + 1.75 \frac{\rho_g \varepsilon_s |u_g - u_s|}{d_p}$$ (2.10)

When $\varepsilon_g > 0.8$

$$K_{gs} = \frac{3}{4} C_D \frac{\varepsilon_s \varepsilon_g \rho_g |u_g - u_s|}{d_p} \varepsilon_g^{-2.65}$$ (2.11)

Where C_D is the drag coefficient proposed by Wen and Yu and is given as

$$C_D = \frac{24}{\varepsilon_g R_{ep}} \left[1 + 0.15 \left(\varepsilon_g R_{ep} \right)^{0.687} \right] \qquad \text{When } R_{ep} \leq 1000$$ (2.12)

$$C_D = 0.44 \qquad \text{when } R_{ep} \geq 1000$$ (2.13)

The particle Reynolds number is defined as follows

$$R_{ep} = \frac{\rho_g d_p |u_g - u_s|}{\mu_g}$$ (2.14)

Stress-Strain Tensors:

The term τ_g and τ_s in eq^n (2.6) & (2.7) are the stress-strain tensors of gas and solid respectively and are given as:-

$$\tau_g = \varepsilon_g \mu_g \left(\nabla u_g + \nabla u_g^T \right) + \varepsilon_g \left(\lambda_g - \frac{2}{3} \mu_g \right) \nabla u_g I \tag{2.15}$$

$$\tau_s = \varepsilon_s \mu_s \left(\nabla u_s + \nabla u_s^T \right) + \varepsilon_s \left(\lambda_s - \frac{2}{3} \mu_s \right) \nabla u_s I \tag{2.16}$$

Solid Pressure:

The pressure gradient produced in solid phase, resulting from normal stresses due to particle – particle interaction. This is very important when solid fraction reaches to a maximum packing. To calculate solid phase pressure gradient, two methods is used i.e. constant viscosity model (CVM) and kinetic theory granular flow (KTGF). In constant viscosity model, the solid phase pressure is only function of local solid porosity using empirical correlations and dynamic shear viscosity of the solid phase is assumed to be constant. And the second model i.e. kinetic theory granular flow (KTGF) is based on the application of the kinetic theory of dense gases. This model gives more idea about particle – particle interaction. In the present work kinetic theory granular flow model has been used.

Closure laws of turbulence:

The effect of turbulent fluctuations of velocity is described by standard k - ϵ model equation. There are three methods used for modeling the turbulence in multi-phase. Those are (i) mixture

turbulence model (ii) dispersed turbulence model (iii) turbulence model for each phase. In the present work, k - ϵ dispersed turbulent model has been used for modeling of turbulence.

The value k and ϵ in gas phase i.e.in continuous phase is directly calculated from differential transport equation. The turbulence kinetic energy in gas phase is representing as follows:

$$\frac{\partial}{\partial x}(\rho_g k_g) + \nabla(\rho_g k_g u_g) = \nabla\left[\left(\mu + \frac{\mu_{t,g}}{\sigma_k}\right)\nabla k_g\right] + G_{k,g} - \rho_g \varepsilon_g + S_k \qquad (2.17)$$

Where σ_k = turbulent kinetic energy

   G_k = generation of turbulence kinetic energy due to mean velocity gradients

   S_k = User- defined source term $= \rho_g \Pi_{kg}$

The Π_{kg} represent the influence of dispersed phase in continuous gas phase. This can be derived from instantaneous equation of continuous phase and Π_{kg} is calculated as below

$$\Pi_{kg} = \sum_{j=1}^{j} \frac{k_{jg}}{\varepsilon_g \rho_g}\left(k_{jg} - 2k_g + u_{jg} * u_{dr}\right) \qquad (2.18)$$

 Where k_{jg}= covariance velocity of continuous gas phase and j represent no of secondary phases.

u_{jg} = relative velocity

u_{dr} = drift velocity

The turbulence dissipation rate in gas phase is representing as follows:

$$\frac{\partial}{\partial x}(\rho_g \varepsilon_g) + \nabla(\rho_g \varepsilon_g u_g) = \nabla\left[\left(\mu + \frac{\mu_{t,g}}{\sigma_\varepsilon}\right)\nabla \varepsilon_g\right] + \frac{\varepsilon_g}{k_g}\left(C_{1g} G_{k\,g}\right) - C_{2\,\varepsilon}\,\rho\frac{\varepsilon_g^2}{k_g} + S_k \qquad (2.19)$$

Then σ_ε= turbulent dissipation energy

S_k= User- defined source term

$S_k = \rho_g \Pi_{\varepsilon g}$ and $\Pi_{\varepsilon g}$ can be calculated as follows

$$\Pi_{\varepsilon g} = C_{3\,\varepsilon}\frac{\varepsilon_g}{k_g}\Pi_{kg} \qquad (2.20)$$

Bahramian et al. (2010) explained the Computational Fluid Dynamics (CFD) modeling of gas-solid, two phase flow and the effect of boundary conditions for predicting the hydrodynamic characteristics of fluidized beds. The hydrodynamics of conical fluidized bed containing dried TiO_2 nano-agglomerates were studied by them both experimentally and computationally. The Eulerian-Eulerian multiphase model and granular kinetic theory using Gidaspow drag function were applied in simulations. The effect of three different types of boundary conditions (BC) including no-slip/friction, free-slip/no-friction and high-slip/small-friction were developed in Schaeffer and Johnson and Jackson were investigated.

Hamzehei et al. (2010) investigated hydrodynamics of a 2D non-reactive gas–solid fluidized bed reactor applying CFD techniques. A multi fluid Eulerian model incorporating the kinetic theory for solid particles was applied to simulate the unsteady state behavior of this reactor and momentum exchange coefficients were calculated by using the Syamlal-O'Brien drag functions and finite volume method was applied to discretize the equations. Simulation results also indicated that small bubbles were produced at the bottom of the bed. These bubbles collided with each other as they moved upwards forming larger bubbles. The effects of particle size and superficial gas velocity on hydrodynamics were also studied.

Sau et al. (2011) carried out experimental and numerical studies for the hydrodynamics in a gas–solid tapered fluidized bed. The experimental results were compared with CFD simulation results. The gas–solid flow was simulated using the Eulerian – Eulerian model and applying the kinetic theory of granular flow for solid particles. The Gidaspow drag model was used to calculate the gas–solid momentum exchange coefficients.

Taghipour et al. (2005) studied experimentally and computationally hydrodynamics of a two-dimensional gas–solid fluidized bed reactor. A multi fluid Eulerian model incorporating the kinetic theory for solid particles was applied to simulate the gas–solid flow. Momentum exchange coefficients were calculated using the Syamlal–O'Brien, Gidaspow and Wen–Yu drag functions. The solid-phase kinetic energy fluctuation was characterized by varying the restitution coefficient values from 0.9 to 0.99.

Goldschmidt et al. (2001) applied two-dimensional multi fluid Eulerian CFD model with closure laws according to the kinetic theory of granular flow to study the influence of the coefficient of restitution on the hydrodynamics of dense gas-fluidized beds. It is observed that hydrodynamics of dense gas- fluidized beds (i.e. gas bubbles behaviors) strongly depend on the amount of energy dissipated in particle-particle encounters.

Fixed bed	Incipiently fluidized bed	Smooth fluidized bed	Bubbling fluidized bed	Turbulent fluidized bed	Channeling fluidized bed	Slugging fluidized bed	Spouted bed
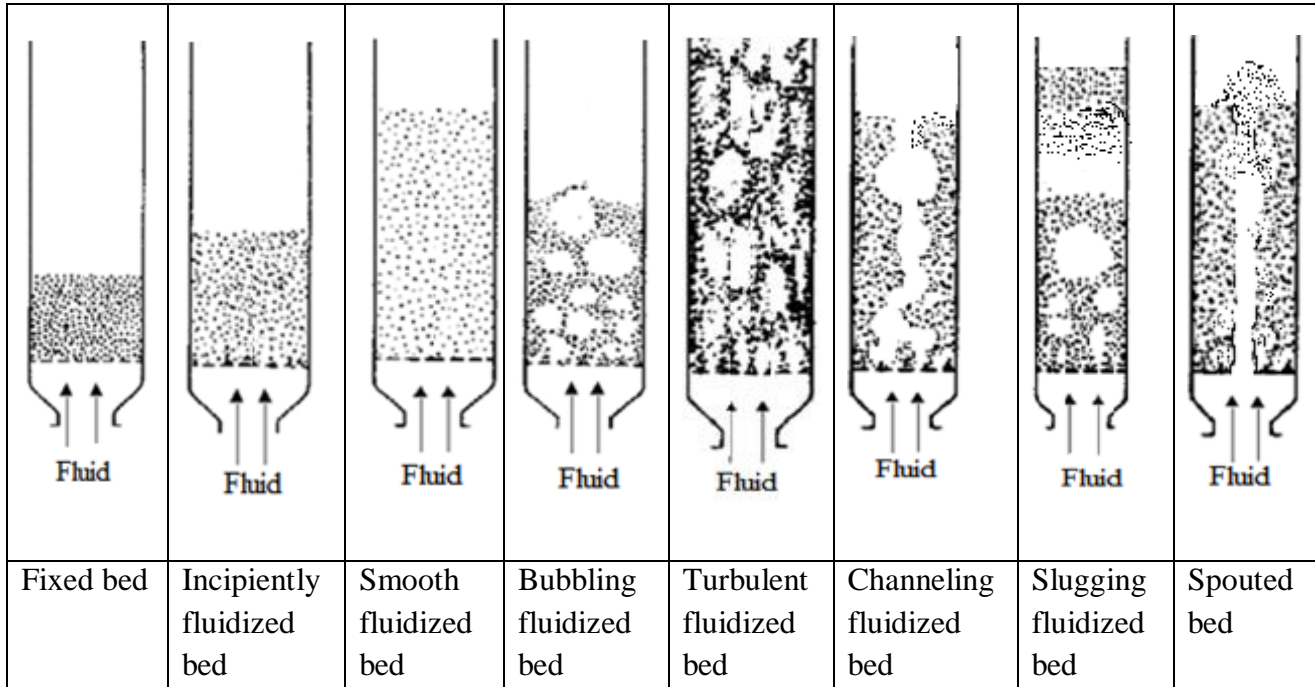
Figure 2.1: Phase Transition with Increasing Gas Flow

Fluidized Bed	Spouted Bed
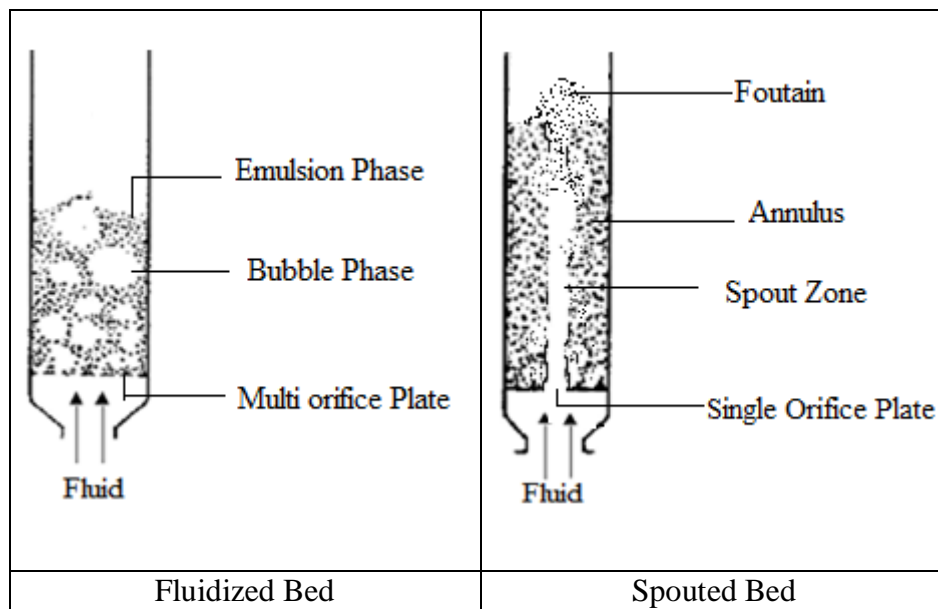
Figure – 2.2: Different Regions of Fluidized / Spouted Bed

CHAPTER –3

EXPERIMENTATION

EXPERIMENTATION

Different sized solid particles (i.e. 5 mm to 70 nm) been analyzed in fluidized / spouted bed. Hydrodynamic studies of these particles have been studied by varying different system parameters. Schematic diagram of experimental set up for spouting process is shown in **Fig. – 3.1**, which consists of number of components.

3.1 Components of Experimental Set-Up

Different components of the experimental set-up are as follows:

1. Air Compressor:

It is a multistage air compressor of sufficient capacity 25 kgf/cm^2.

2. Air Accumulator / Receiver:

It is a horizontal cylinder used for storing the compressed air from compressor. There is one G.I. pipe inlet to the accumulator and one by-pass line from one end of the cylinder. The exit line is also a G.I. pipe taken from the central part of the cylinder. The purpose of using the air accumulator in the line is to dampen the pressure fluctuations. The operating pressure in the cylinder is kept at 20 psig.

3. Pressure Gauge:

A pressure gauge in the required range (1-50 psig) is fitted in the line for measuring the working pressure. The pressure gauge is fitted with an air accumulator / receiver.

4. Silica Gel Tower:

A silica gel tower is used for absorbing the moisture content of the air supply. A silica gel column is provided in the line immediately after the air receiver to arrest the moisture carried by air from the receiver / air accumulator.

5. Valves:

A globe valve of ½ inch ID is provided in the by-pass line for sudden release of the line pressure. A gate valve of 1/2 inch ID is provided in the line just before rotameter to control the flow rate of air to the fluidizing bed.

6. Rotameter:

A Rotameter is used in the line for measuring the flow rate of the air i.e. used as fluidizing medium. The Rotameter used in the range of 0-50 m^3/ hr for spouting purpose and 0 -10 lpm for fluidizing purpose.

7. Air Calming Section:

This is an important component of the experimental set-up. It consists of a cylindrical portion (4.5 cm id. and 7.5 cm length) followed by a conical bottom. The cone angle is about 35^0- 40°. The larger side is of 45 mm id. and the smaller of 12 mm id., the height of the cone being 6.5 cm. The cone is brazed with G.I. flange of 11.4 cm O.D. The central bore of the flange is also of 45 mm dia. The cone is made of ordinary G.I. sheet. The inside hollow space of the distributor is filled with spherical glass beads of size 5 mm for uniform distribution of fluid for

fluidizing purpose and without packing of spherical glass beads used for spouting purpose for uniform distribution of fluid to avoid channeling.

8. Air Distributor:

For spouting process, a card board of circular size was used as the distributor, made up of 4mm thick card board which was strong enough to withstand the air pressure. It was easy to make hole in this distributor by simply cutting at the centre. For fluidization process a filter cloth placed on a perforated plate made up of G.I sheet is used as the air distributor. Orifices on this plate are of 5 mm openings and randomly placed.

9. Fluidizer:

The fluidizers are cylindrical columns made up of transparent Perspex sheets column with one end fixed to a Perspex flange. The flange of 5/16" thickness has 4 bolt holes of ¼" dia. Two pressure tapings are provided for noting the bed pressure drop. A screen is provided at the bottom of the flange and the conical claiming section is also attached with the flange of the fluidizer.

10. Manometer Panel Board:

A U tube manometer is used to measure the bed pressure drop. Mercury used as the manometric liquid for spouting whereas carbon tetra chloride for fluidization purpose.

3.2 Procedure for Coarse (Irregular / Regular) Particles

Initially, the material is taken in the fluidizer, the bed height is noted. Air is passed through the bed; the expanded bed height is noted with the increased flow rate of air. Bed expansion / fluctuation, pressure drop was measured at each velocity. The fluidizer is a cylindrical column of diameter, 10 cm and length 100 cm. An 80 mesh screen is placed just above the distributor plate between the lower flange of the fluidizer and the conical air distributor to prevent the backflow of bed materials. This is tightly attached to the column with the help of a gasket, so that there is no leakage of air.

The calming section was without any packing material for spouted bed for allowing a jet of fluid to pass through the central hole of the distributor. The spout diameter was varied as 2.5 cm, 3 cm, 3.5 cm and 4 cm for coarse regular/ irregular particles. Air flow rate was measured with Rotameter and U-tube manometer was used for measuring the pressure drop across the bed with the mercury (Hg) as the manometric fluid.

The same procedure was repeated for different spout diameter for different static bed heights and different particle sizes/ densities of bed materials. Thus the variations of different system parameters are discussed as scope of the experiment in **Table – 3.1 (A)** and **(B)**. The bed dynamics (i.e. bed expansion / fluctuation ratio, fluidization index) can be calculated by using eq^n 2.1, 2.2 and 2.3 for developing correlations.

3.3 Procedure for Fine Particles in spouted bed

Different fine particles were used to study the bed dynamics in same experimentation unit (**Fig. -3.1**) was used but only the fluidizer was changed. The fluidizer was a cylindrical column (made up of Perspex material) of diameter, 5 cm and length 100 cm. A filter cloth is between the lower flange of the fluidizer and the calming section to prevent the backflow of bed materials. Air distributer is used above the filter cloth. This is tightly attached to the column with the help of a gasket, so that there is no leakage of air. No packing material was used in the calming section. Air distributor was prepared from card boards by making a hole at the centre which is known as the spout and the dia. of spout was also varied i.e. 1 mm, 2mm, 3 mm, and 4mm.

The experiments were carried out by allowing air to flow through the distributor by varying the different system parameter and are discussed as scope of the experiment in **Table – 3.2**. The expanded bed heights and manometer readings were noted down at different flow rates of the supplied air under different operating conditions.

For Fluidization Process:-

Hydrodynamics studies of different sized solid particles in fluidized bed were also carried out in the same experimental set up (**Fig.- 3.1**), only distributor and fluidizer was changed and a rod promoter used.

3.4 Procedure for Fine Particles

The fluidizer is a cylindrical column (made up of Perspex material) of diameter 5 cm and length 100 cm. A filter cloth (orifice ≈ 40 microns) is placed between the lower flange of the fluidizer and the calming section to prevent the backflow of bed materials. This is tightly

attached to the column with the help of a gasket, so that there is no leakage of air. The calming section was packed with glass beads for allowing the fluid to pass through filter cloth of the distributor and carbon tetra chloride (CCl_4) as the manometric fluid.

During fluidization process a stirrer (a rod promoter) was hanged from the top of the fluidized column to vibrate the bed as shown in **Fig. - 3.2**. The stirrer was connected to a motor and speed of rotation was varied by a Varriac. Six numbers of rods each of 6 mm diameter were used. Five numbers of rods were placed laterally having 75 mm length and spacing of 60 mm between two successive rods & length of central rod is 350 mm. Fluidizer with the stirrer is shown in **Fig.–3.3**.

The experiments were carried out by passing air through the distributor by varying the different system parameter and are discussed as scope of the experiment in **Table -3.3**. The expanded bed heights and manometer readings were observed at different flow rates of the supplied air.

3.5 Procedure for Nano Materials

Hydrodynamic studies of nano particles were also carried out in the same experimental set up as **Fig. -3.1**, only fluidizer was changed. An arrangement was made for applying external force on the outer surface of the column. One, central rod of 6 mm diameter and 350 mm long was used for the stirrer. Five numbers of rubber tubes, each of 75 mm length and spaced at a distance of 60 mm from the other were placed laterally (**Fig.–3.2**). The Stirrer is placed just outside the column to exert external radial force on the column. Fluidizer with the stirrer is shown in **Fig. – 3.3**.

The experiments were carried out by varying the different system parameter and are discussed as scope of the experiment in **Table – 3.4**. The expanded bed heights and manometer readings were noted down at different flow rates of the supplied air under different operating conditions.

Table – 3.1 (A): Scope of Experiment for Coarse Irregular Particles in Spouting Process

SL.NO.	MATERIALS	H_S, cm	d_p, mm	D_i, cm	ρ_s, g/cc	U_0/U_{mf}
1	Dolomite	8	3.325	2.5	2.89	1
2	Dolomite	12	3.325	2.5	2.89	1
3	Dolomite	16	3.325	2.5	2.89	1
4	Dolomite	20	3.325	2.5	2.89	1
5	Dolomite	8	2.58	2.5	2.89	1
6	Dolomite	8	2.18	2.5	2.89	1
7	Dolomite	8	1.7	2.5	2.89	1
8	Dolomite	8	3.325	3	2.89	1
9	Dolomite	8	3.325	3.5	2.89	1
10	Dolomite	8	3.325	4	2.89	1
11	Brick	8	3.325	2.5	1.92	1
12	Marble	8	3.325	2.5	1.39	1
13	Coal	8	3.325	2.5	1.57	1
14	Dolomite	8	3.325	2.5	2.89	1.1
15	Dolomite	8	3.325	2.5	2.89	1.2
16	Dolomite	8	3.325	2.5	2.89	1.3

Table – 3.1 (B): Scope of Experiment for Coarse Regular Particles inSpouting Process

SL.NO	MATERIALS	H_S, cm	d_p, mm	D_i, cm	ρ_s, g/cc	U_0/U_{mf}
1	Glass Beads	8	3.325	2.5	2.8	1
2	Glass Beads	12	3.325	2.5	2.8	1
3	Glass Beads	16	3.325	2.5	2.8	1
4	Glass Beads	20	3.325	2.5	2.8	1
5	Glass Beads	8	2.58	2.5	2.8	1
6	Glass Beads	8	2.18	2.5	2.8	1
7	Glass Beads	8	1.7	2.5	2.8	1
8	Glass Beads	8	3.325	3	2.8	1
9	Glass Beads	8	3.325	3.5	2.8	1
10	Glass Beads	8	3.325	4	2.8	1
11	Aluminum Balls	8	3.325	2.5	3.21	1
12	Mustard Seeds	8	3.325	2.5	1.3	1
13	Sago	8	3.325	2.5	1.59	1
14	Glass Beads	8	3.325	2.5	2.8	1.1
15	Glass Beads	8	3.325	2.5	2.8	1.2
16	Glass Beads	8	3.325	2.5	2.8	1.3

Table – 3.2: Scope of Experiment for Fine Particles in Spouting Process

SL.NO.	MATERIALS	H_S, cm	d_p, microns	D_i, mm	ρ_s, g/cc	U_0/U_{mf}
1	Dolomite	8	63	3	1.15	1
2	Dolomite	12	63	3	1.15	1
3	Dolomite	16	63	3	1.15	1
4	Dolomite	20	63	3	1.15	1
5	Dolomite	8	125	3	1.15	1
6	Dolomite	8	90	3	1.15	1
7	Dolomite	8	45	3	1.15	1
8	Dolomite	8	63	1	1.15	1
9	Dolomite	8	63	2	1.15	1
10	Dolomite	8	63	4	1.15	1
11	Alumina	8	63	3	0.64	1
12	Marble	8	63	3	1.39	1
13	Sand	8	63	3	1.14	1
14	Dolomite	8	63	3	1.15	1.25
15	Dolomite	8	63	3	1.15	1.5
16	Dolomite	8	63	3	1.15	1.75

Table – 3.3: Scope of the Experiment for Fine Particles in Fluidization Process

S.L. No	MATERIALS	U_o/U_{mf}	H_s, cm	N, rpm	ρ_s, g/cc	d_p, μm
1	Talcum Powder	1.25	16	121.2	0.88	80
2	Talcum Powder	1.5	16	121.2	0.88	80
3	Talcum Powder	1.75	16	121.2	0.88	80
4	Talcum Powder	2.0	16	121.2	0.88	80
5	Talcum Powder	1.25	20	121.2	0.88	80
6	Talcum Powder	1.25	24	121.2	0.88	80
7	Talcum Powder	1.25	28	121.2	0.88	80
8	Talcum Powder	1.25	16	73.9	0.88	80
9	Talcum Powder	1.25	16	101.6	0.88	80
10	Talcum Powder	1.25	16	137.4	0.88	80
11	Alumina Powder	1.25	16	121.2	0.64	63
12	Silicon Carbide	1.25	16	121.2	0.72	70
13	Magnetite	1.25	16	121.2	2.4	75
14	Talcum Powder	1.25	16	121.2	0.88	80
15	Talcum Powder	1.25	16	121.2	0.88	80
16	Talcum Powder	1.25	16	121.2	0.88	80

Table – 3.4: Scope of the Experiment for Nano Particles in Fluidization Process

SL. No.	Static bed height (H_s),cm	Superficial air velocity (U_0), m/s	Angular velocity (ω), rpm	External force (F), N
1	8	0.084	277	2.83
2	12	0.093	335	3.43
3	16	0.101	411	4.2
4	20	0.11	575	5.88

1. Compressor; 2. Receiver; 3.Constant pressure tank; 4. Pressure gage; 5. Silica gel tower; 6. By pass valve; 7. Line valve; 8.Rotameter;   9.Calming section without   glass bead packing;   10.Fluidizer; 11.Distributer; 12.Pressure tapping 13.U tube manometer (Hg columns)
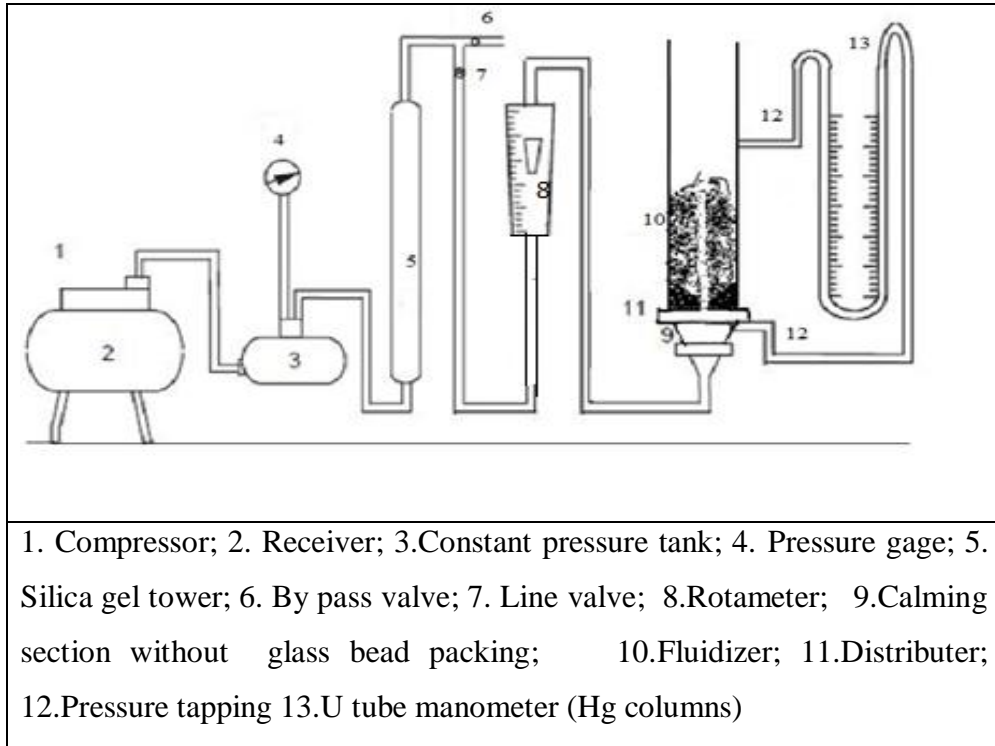
Figure – 3.1: Schematic View of the Experimental Set-up
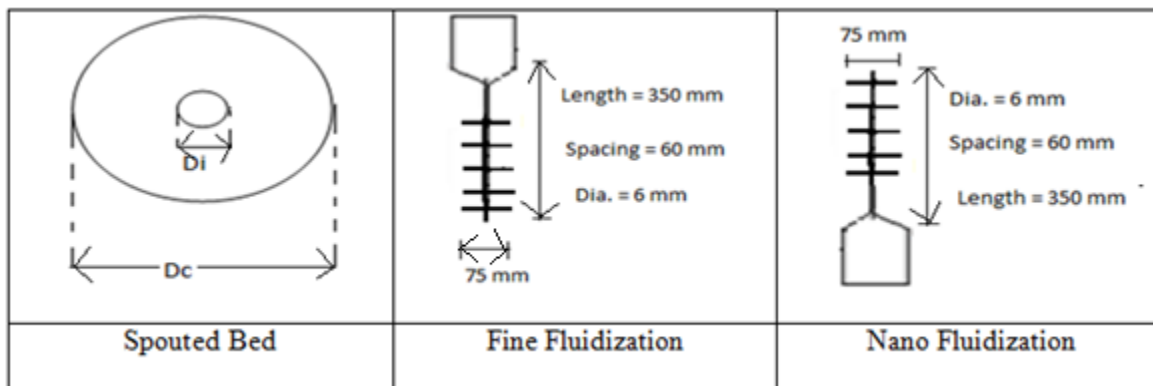
Figure – 3.2: Schematic Diagram Distributor and Stirrer
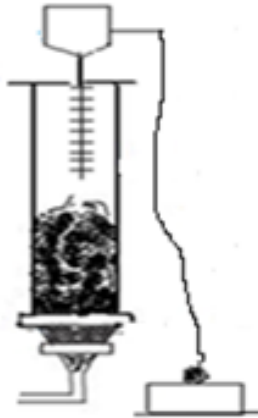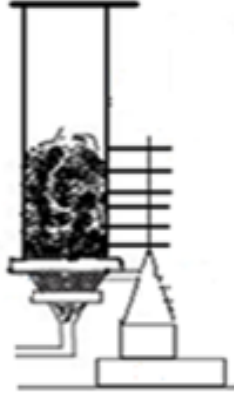
| Spouted Bed | Fine Fluidization | Nano Fluidization |

Figure – 3.3: Schematic Diagram and Picture of the Fluidizers

CHAPTER – 4

HYDRODYNAMIC STUDIES

HYDRODYNAMIC STUDIES

The hydrodynamic study of the fluidized / spouted bed has been carried out by analyzing the bed dynamics for coarse (regular/ irregular), fine and nano particles.

The following bed dynamics were analyzed in a spouting / fluidization processes are

- Minimum Fluidization(U_{mf}) / Spouting Velocity (U_{ms})

- Pressure Drop (Δp)
- Bed Expansion Ratio (R)

- Bed Fluctuation Ratio (r)
- Fluidization Index (FI)

4.1: Coarse (Regular / Irregular) Particles in Spouted bed:-

4.1.1 Pressure drop and minimum spouting velocity

The overall changes in values of bed pressure drops of coarse (regular / irregular) particles were observed to increase with the increase in superficial spout velocity (U_o) for the spouted bed (**Fig.- 4.1**).

In spouting process, the bed pressure drop gradually increases with increase in spouting velocity up to certain limit and then decreases up to certain point after which it remains constant. The reasons behind this may be due to the following facts:

i.   Initially at low air flow rates, the air simply passes up without disturbing the solid particles. The pressure drop is observed to be a linear function of the air flow rate showing packed bed behavior.

ii. Again with the increase in air flow rate to a certain value, an empty cavity is formed just above the inlet at the base of the bed. The particles surrounding the cavity are

compressed and form a compacted arch which offers a greater resistance to flow. As a result the total pressure drop across the bed continues to rise.

iii. With further increase in air flow, the cavity elongates to form an internal spout and the arch of compacted solids still exists above the internal spout so that the pressure drop across the bed rises further until it reaches a maximum value.

iv. As the air flow rate is increased further, the height of the hollow internal spout becomes large in comparison with the packed solids i.e. the resistance offered by the arched solids is exceeded by air velocity and fountain forms then the pressure drop decreases to a certain point. Further increase in air flow rate, breaks the spout causing the fluidization of solids for which the pressure drop remains constant, the corresponding velocity at which the pressure drop is constant is called as the minimum spout velocity.

In case of coarse irregular, the bed pressure drop increases sharply with increase in spouting velocity as compared to coarse regular particles. This is due to the presence of more number of air bubbles in coarse irregular particles. Thus the bed pressure drop increases with increase in superficial velocity of air as size of air bubble also increases.

4.1.2 Bed Expansion Ratio

The values of bed expansion ratio of coarse (regular/ irregular) particles are also observed to increase with the increase in superficial velocity (U_o) for spouted bed (**Fig. – 4. 2**).

This may be due to the fact that when superficial velocity exceeds minimum spout velocity. As a result more number of air bubbles forms thereby causing bed expansion. As air

bubble size increases with increase in spouting velocity, the bed expansion ratio increases. Again with increase in initial static bed height (H_s) and spout diameter (D_i) the bed expansion ratio are observed to decrease. This may be due to the breaking up of air bubbles with increase in initial static bed height. The bed expansion ratio is also observed to increase with the increased density of the particles (ρ_s), and the increased particle sizes (d_p).

In case of irregular coarse particles, bed expansion ratio is observed to be more in comparison with coarse regular particles. This may be due to the presence of more number of air bubbles with irregular particles. Thus the initial height for irregular particles expands more as compared to regular coarse particles.

4.1.3 Bed Fluctuation Ratio

The values of bed fluctuation ratio for coarse (regular/ irregular) particles are observed to increase with the increase in superficial velocity (U_o) for spouted bed (**Fig. – 4. 3**).

It is observed that with the increase in superficial air velocity (U_o) bed fluctuation ratio increase. Again with an increase in initial static bed height (H_s) and spout diameter (D_i), the bed fluctuation ratios decrease. This may be due to the more weight of bed materials and breaking up of air bubbles with increased initial static bed height which restrict the movement of materials at a constant velocity. The bed fluctuation ratio is also observed to increase with the increased density of the particles (ρ_s). This may be due to the fact that minimum expanded height of bed (H_{min}) reduces to minimum due to heaviness of the particles with increase in density. The bed fluctuation ratio also increase with increased particle size (d_p) decrease in excess gas velocity

because less number of air bubbles present and also minimum expanded height of bed (H_{min}) reduces due to breakage of air bubbles.

In case of irregular coarse particles, bed fluctuation ratio is more as compared to regular particles. This may be due to the breakage of more number of bubbles with irregular particles as a result the minimum expanded height of bed (H_{min}) reduces thereby increasing the bed fluctuation ratio.

4.1.4 Fluidization Index

The fluidization index of coarse (regular/ irregular) particles is observed to increase initially with the increase in superficial velocity (U_o) for spouted bed (**Fig. - 4.4**) upto certain point then decreases suddenly and after that it remains constant.

A high value of fluidization index is observed for glass beads, marble and bricks implying that the bed can hold more gas between the minimum fluidization and bubbling point. A low value of fluidization index is observed for the mustard seeds, sago and coal implying that less gas is held between the minimum fluidization and bubbling point, because of less bubble formation among particles. The fluidization index of aluminium balls and dolomite is approximately one indicating the case of ideal fluidization.

In case of irregular coarse particles, fluidization index is more as compared to coarse regular particles. Profile of fluidization index is similar to that of bed pressure drop for spouted bed (**Fig. – 4.4**). The bed pressure drop is more in irregular particles than the coarse regular particles because of the surface irregularities.

4.2: For Fine Fluidization / Spouting Process:-

The hydrodynamic study of the fluidized or spouted bed using fine particles has been carried out thereby analysing the bed pressure drop, bed expansion and / or fluctuation ratio and fluidization index.

4.2.1 Pressure drop and Minimum Spouting/ Fluidization Velocity

The bed pressure drop of fine particles is observed to increase with the increase in superficial velocity (U_o) for both, the fluidized bed and spouted bed (**Fig. - 4. 5**).

It is observed that the bed pressure drop gradually increases with increase in superficial gas velocity up to certain limit after which it remains constant when all the bed materials are fluidized. In the case spouting process, it is observed that with the increase in gas flow, the bed pressure drop gradually increases up to certain limit because air simply passes up and an empty cavity/ spout formed at the inlet of the bed. Again increasing air flow rate, the bed pressure drop decreases up to certain point after which it remains constant. In this case, spout breaks and all the bed materials are in fluidization condition.

4.2.2 Bed Expansion Ratio

The bed expansion ratio of fine particles is observed to increase with the increase in superficial gas velocity (U_o) for both, the fluidized bed and spouted bed (**Fig. – 4. 6**).

This may be due to the fact that when superficial gas velocity exceeds minimum fluidisation / spouting velocity. As a result more number of gas bubbles forms thereby causing bed expansion and the gas bubble size increases with excess superficial gas velocity. Again with

increase in initial static bed height (H_s) the bed expansion ratio is observed to increase and decrease for fluidized bed and spouted bed respectively. The reason may be frequent breakage of more number of air bubbles in the spouted bed whereas in fluidized bed bubble size increases. For fluidized bed, the bubbles grow in sizes with the increased superficial velocity of fluid causing higher bed expansion. But for the spouted bed, the bubbles breaks easily by the spout of fluid with increased superficial velocity thereby decreasing the bed expansion.

The bed expansion ratio is observed to be decreases with the increased speed of the stirrer (N) and increased spout diameter (D_i). This may be due to the bed materials of column moves vigorously and the air bubbles are break due to collision among particles. As a result the bed expansion decreases with in cease of speed of stirrer and dia. of spout. The bed expansion ratio is also observed to increase in both cases with the increased density of the particles (ρ_s) as when density increases minimum fluidization / spout velocity increases and the bed expansion ratio increases accordingly. Similarly increased particle size (d_p) increases the bed expansion for both the cases.

4.2.3 Bed Fluctuation Ratio

The bed fluctuation ratio of fine particles is observed to increase with the increase in superficial gas velocity (U_o) for both, the fluidized bed and spouted bed (**Fig. – 4.7**).

This may be due more gas bubbles formed when superficial gas velocity exceeds minimum fluidisation / spouted velocity. Again with increase in initial static bed height (H_s), the bed fluctuation ratio increases for both cases. This may be due to the minimum expanded bed height (H_{min}) reduces to minimum due to heaviness of the particles thereby increasing the bed

fluctuation ratio. The bed fluctuation ratio are observed to be decreased with the increased speed of the stirrer (N) and increased spout diameter (D_i), due to breaking up of gas bubbles by collision among particles in the bed. Increase in spout diameter allows more air to flow thereby preventing bubble formation. The bed fluctuation ratio is also observed to increase and decrease with the increased density of the particles (ρ_s), for fluidized and spouted bed respectively. Similarly increased particle size (d_p), increases bed fluctuation ratio in both cases due to frequent bubble formation and breakage of air bubbles. As a result minimum expanded bed height (H_{min}) reduces thereby increasing the bed fluctuation ratio.

4.2.4 Fluidisation Index

The fluidization index of fine particles are observed to increase with the increase in superficial gas velocity (U_o) for both, the fluidized bed and spouted bed (**Fig. – 4. 8**).

Fluidization index gives an idea of the degree of the uniformity in expansion of the bed. A high value of fluidization index was observed for sand and silicon carbide powders implying that the bed can hold more gas between the minimum fluidization and bubbling point. A low value of fluidization index is observed for the talcum powder, magnetite and dolomite powder because of more cohesive forces among particles thereby indicating a brittle fluidization state where a small change could cause a break from the uniformly fluidized state to a bubbling regime or a packed bed.

4.3: <u>For Nano Fluidization Process</u>:-

The hydrodynamic behaviours of copper nano materials (i.e. d_p = 70 nm and surface area = $5 m^2/gm$) have been studied in fluidized bed.

4.3.1 Pressure drop and Minimum Fluidization Velocity

The bed pressure drop of copper nano particles are observed to increase with the superficial velocity (U_o) in the fluidized bed as shown in **Fig. - 4.9 (a)**.

It is observed that the bed pressure drop gradually increases with increase in superficial gas velocity. Once the bed is completely fluidized, the bed pressure drop across the bed remains constant, but bed height continues to increase with increasing superficial velocity for nano particles is shown in **Fig. - 4.9(b)**.

4.3.2 Bed Expansion Ratio

The bed expansion ratio of copper nano particles are observed to increases with the increase in superficial gas velocity (U_o), (**Fig. – 4. 10**).

This may be due to the fact that as superficial gas velocity exceeds minimum fluidization velocity, more number of gas bubbles forms thereby causing bed expansion. As bubble size increases further with increase in superficial velocity of fluid, bed expands further**. The bed expansion ratio also increases with the increase in static bed height and decreases on the application of external force (i.e. equivalent centrifugal force)**. This may be due to breakage of gas bubbles in fluidized bed.

4.3.3 Bed Fluctuation Ratio

The bed fluctuation ratio of copper nano particles are observed to increase with the increase in superficial gas velocity (U_o), (**Fig. – 4. 11**).

This may be due to excess velocity above minimum fluidization velocity, as a result more number of bubbles forms and bubble size increases gradually. Application of external force decreases the bed fluctuation ratio due to frequent breaking of air bubbles. Increased external force prevents entrainment and elutriation of particles.

4.3.4 Fluidization Index

The fluidization index of copper nano particles are observed to increase with the increase in superficial gas velocity (U_o), (**Fig. – 4. 12**) upto certain point, then decreases suddenly and after that remains constant.

At low gas velocity, nano particles exhibit only slugging and channeling in a fluidized bed column. With the application of external force, the bed of nano particles fluidized smoothly. It is observed experimentally that on application of external force the fluidization index value is close to one indicating almost ideal fluidization behaviors.
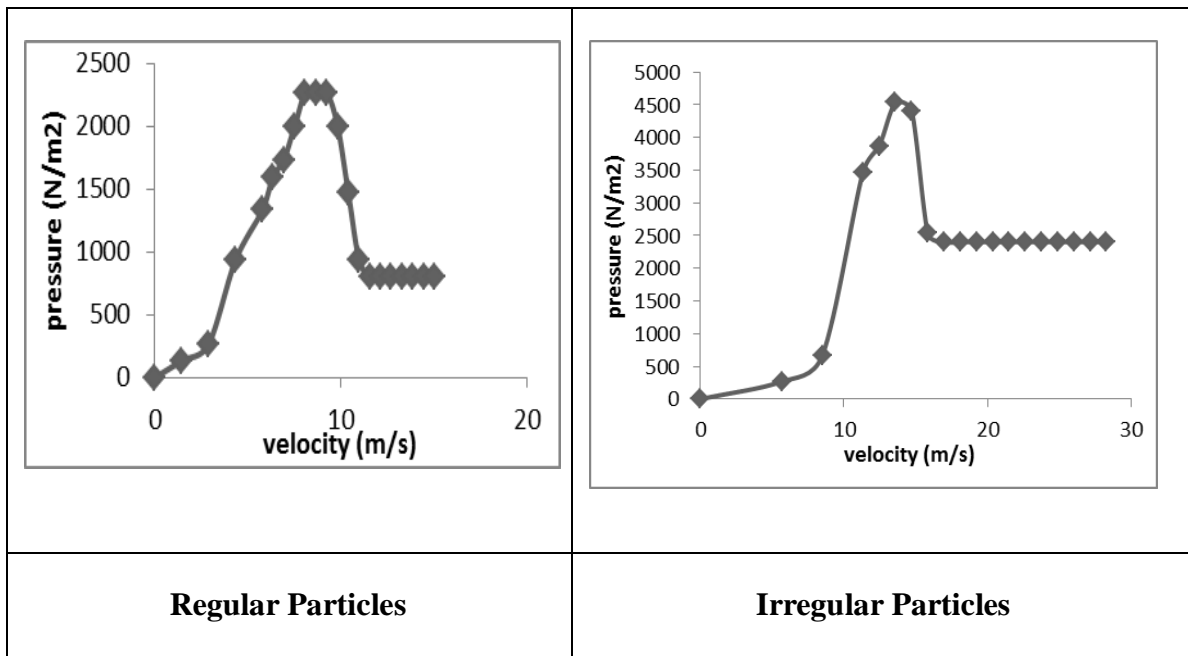
Figure – 4.1: Comparison Plot of Bed Pressure drop Profile for Coarse Particles
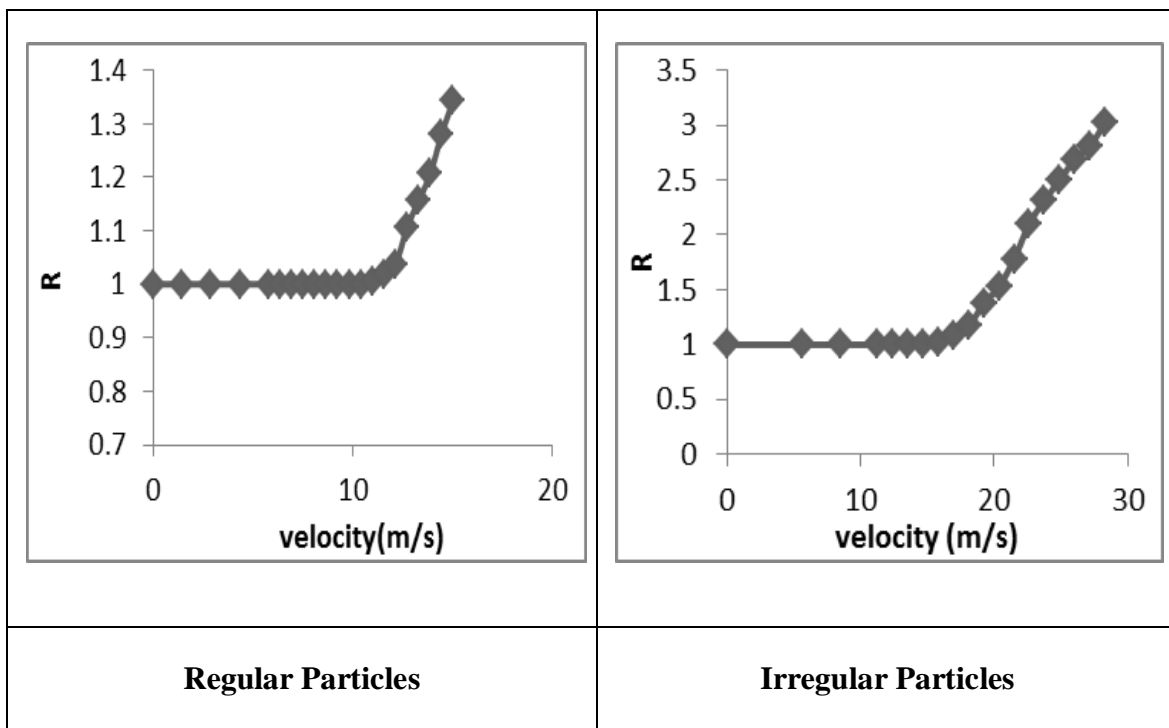
Figure – 4.2: Comparison Plot Bed Expansion Ratio for Coarse Particles

| Regular Particles | Irregular Particles |
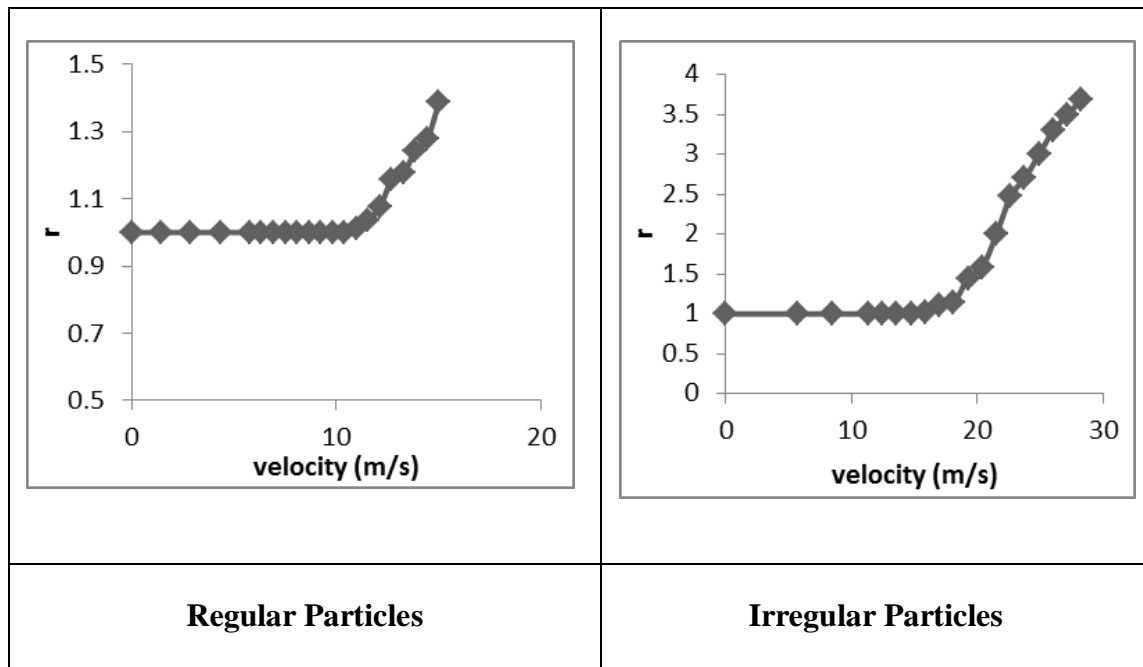
Figure – 4.3: Comparison Plot Bed Fluctuation Ratio for Coarse Particles

| Regular Particles | Irregular Particles |
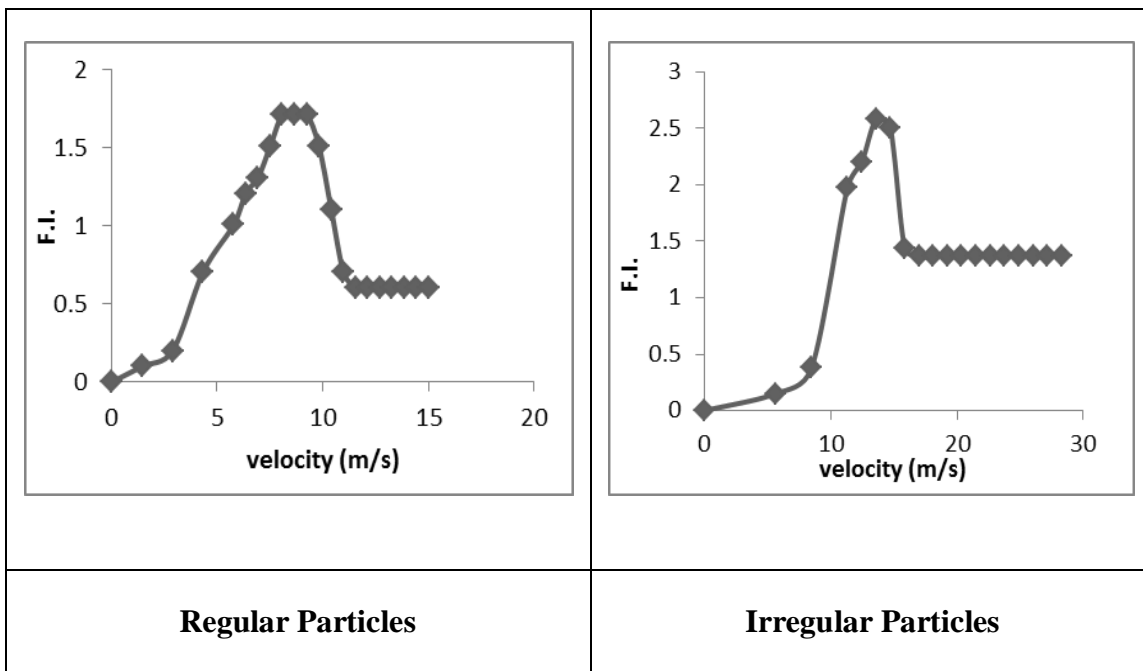
Figure – 4.4: Comparison Plot Fluidization Index for Coarse Particles

| Fluidization Process | Spouting Process |
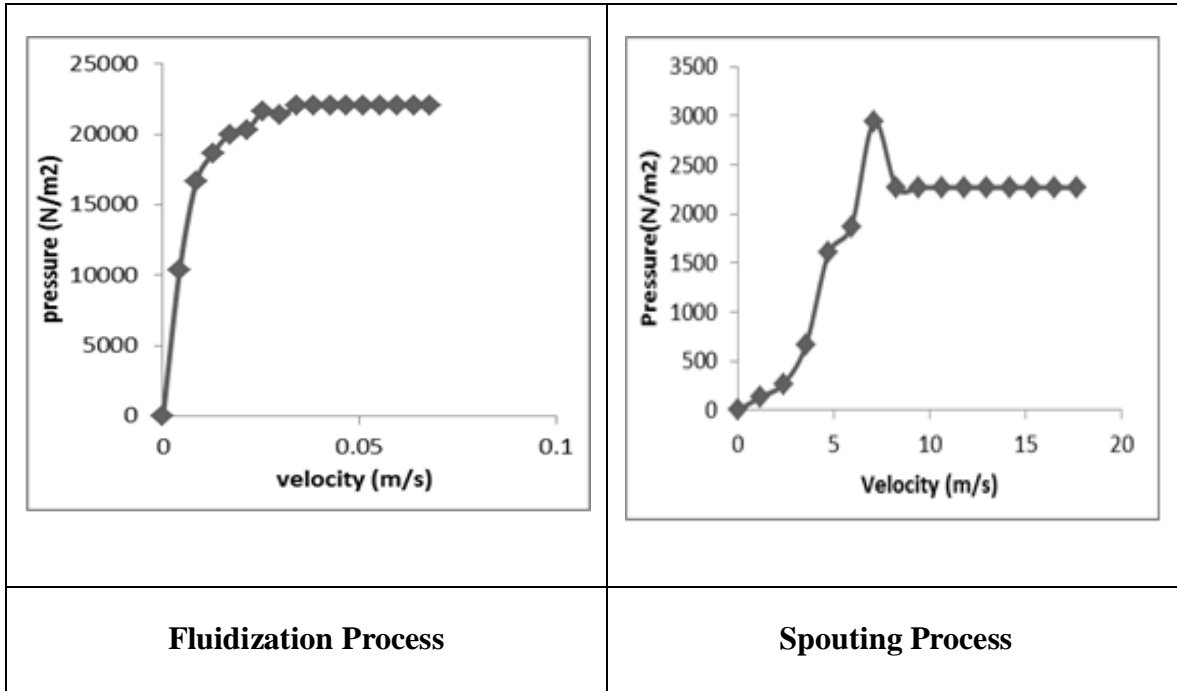
Figure – 4.5: Comparison Plot of Bed Pressure Drop Profile for Fine Particles

| Fluidization Process | Spouting Process |
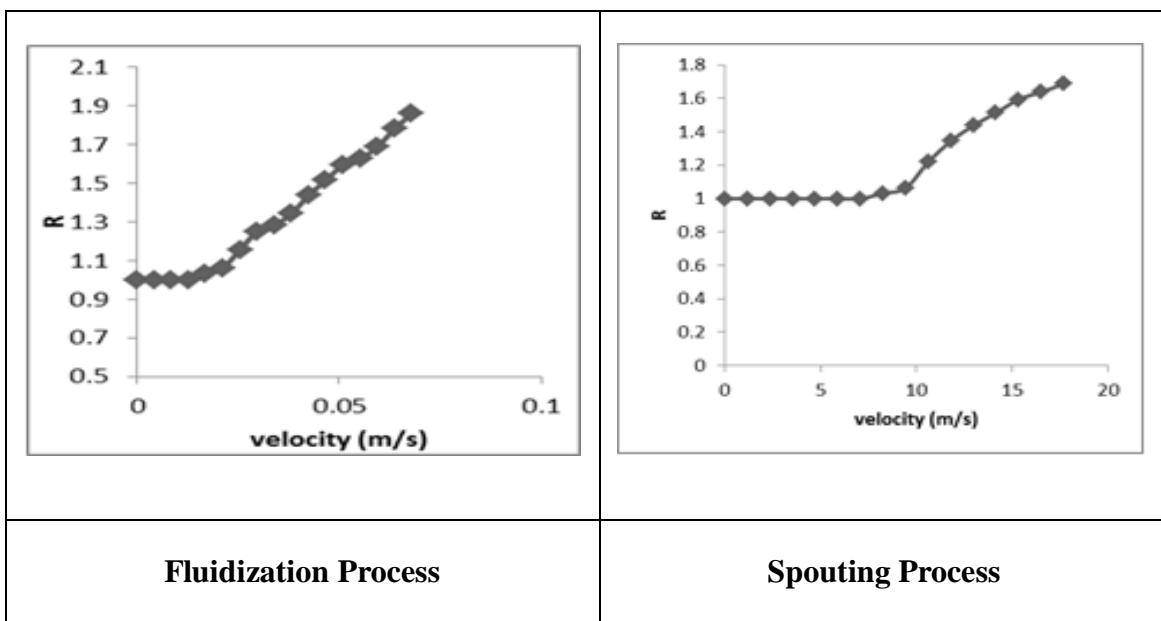
Figure – 4.6: Comparison Plot of Bed Expansion Ratio for Fine Particles

| Fluidization Process | Spouting Process |
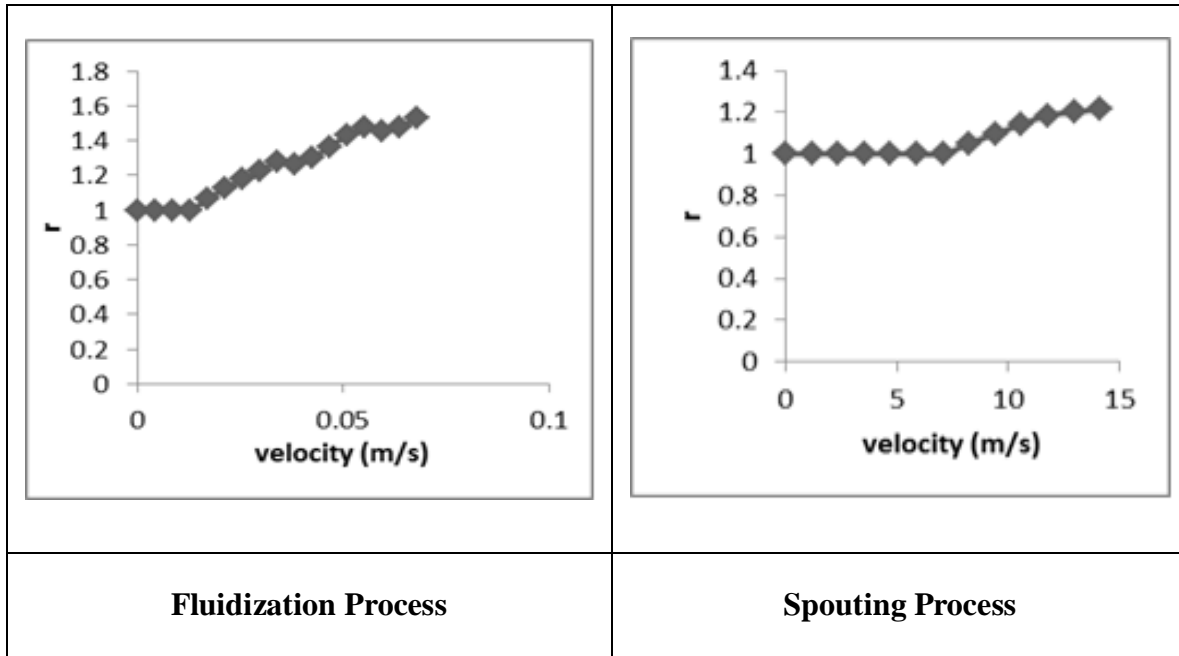
Figure – 4.7: Comparison of Bed Fluctuation Ratio for Fine Particles

| Fluidization Process | Spouting Process |
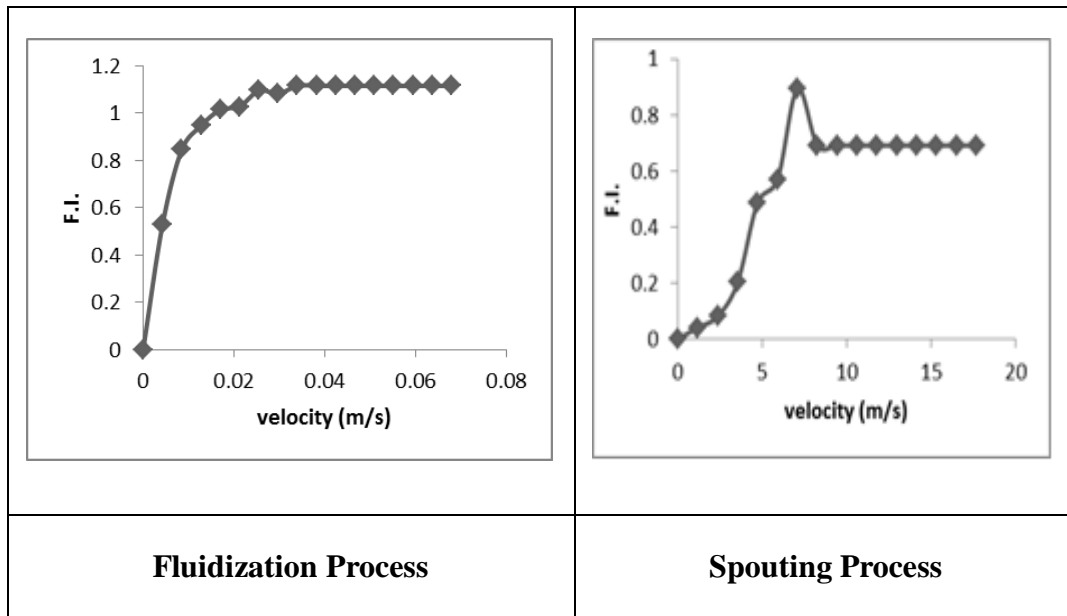
Figure – 4.8: Comparison Plot of Fluidisation Index for Fine Particles

(a) Bed Pressure Drop	(b) Maximum Bed Height
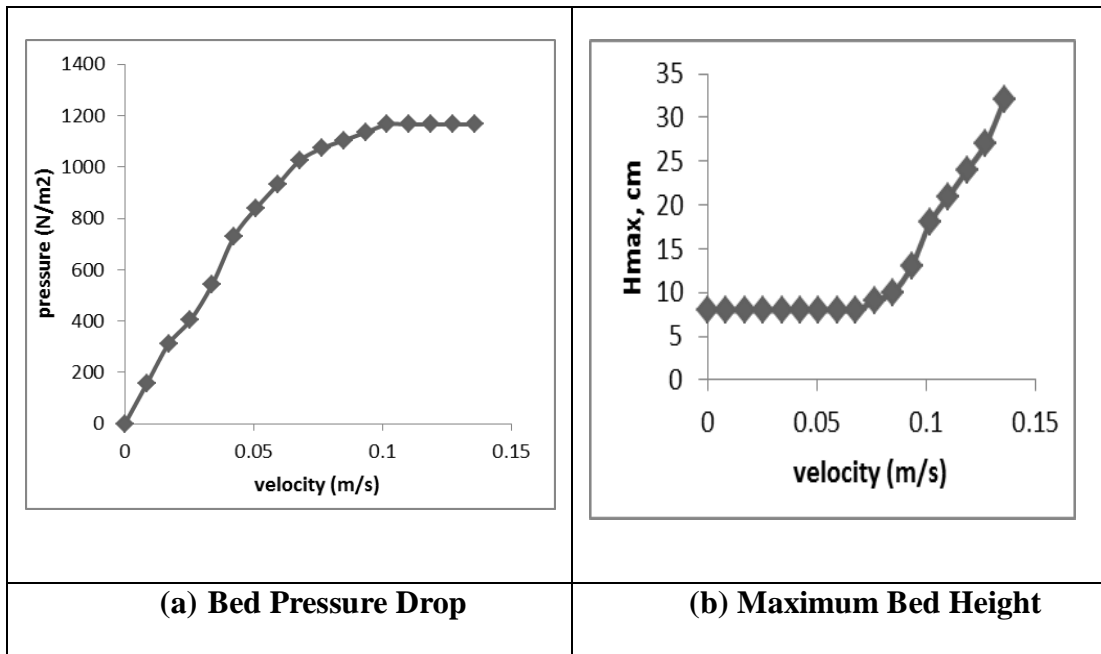
Figure – 4.9: Variation of Pressure Drop/ bed height against Superficial Velocity for Nano Particles
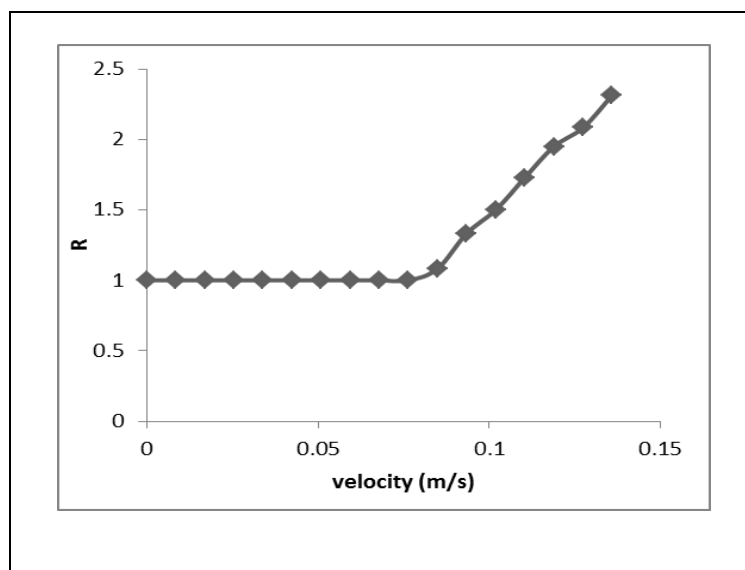
Figure – 4.10: Bed Expansion Ratio against Superficial Velocity for Nano Particles
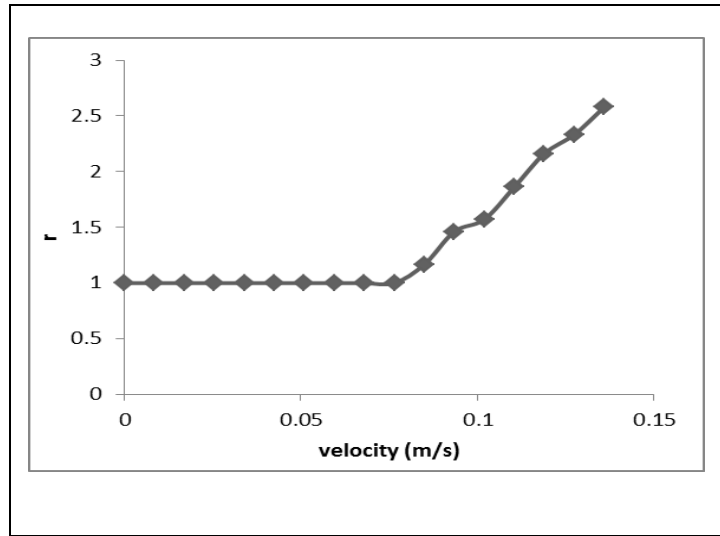
Figure – 4.11: Bed Fluctuation Ratio against Superficial Velocity for Nano Particles
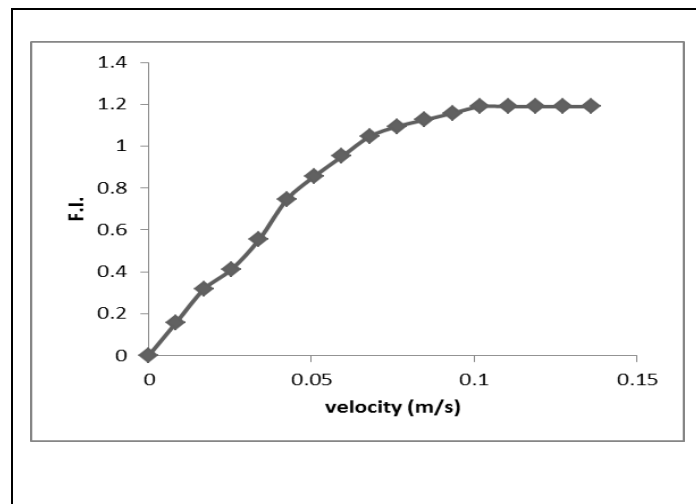
Figure – 4.12: Fluidization Index against Superficial Velocity for Nano Particles

CHAPTER – 5

CFD SIMULATION FOR

HYDRODYNAMIC BEHAVIOUR

CFD SIMULATION FOR HYDRODYNAMIC BEHAVIOUR

5.1 Introduction

Over the past few decades, Computational Fluid Dynamics (CFD) has been used to improve process design by allowing engineers to simulate the performance of alternative configurations, eliminating guesswork that would normally be used to establish equipment geometry and process conditions. The use of CFD enables engineers to obtain solutions for problems with complex geometry and boundary conditions. A CFD analysis yields values for pressure, fluid velocity, temperature, and species or phase concentration on a computational grid throughout the solution domain.

Computational Fluid Dynamics (CFD) is an important tool for design and optimization of chemical processes. A fundamental problem encountered in modeling hydrodynamics of a fluid–solid fluidized bed is the motion of two phases. For the fluidization operation minimum two phases are required; one is called primary phase and other one is secondary phase. Usually the fluid which passes through the inlet is considered as primary phase and particulate in the bed is the secondary phase. The operating conditions like superficial fluid velocity, temperature of the primary and secondary phase, and inlet and exit pressure of the bed affect the performance of the fluidized bed. The physical property of the phases, particle size and distribution controls the hydrodynamic behaviors of it. Hydrodynamic modeling has the remarkable ability to synthesize data from various, relatively simple experiments and, thereby, to describe the time-dependent distribution of fluid and solids volume fractions, velocities, pressure, temperature, and species mass fractions in industrial reactors, where measurement of such quantities might be all but impossible. Such calculations, therefore, allow the designer to visualize the conditions in the

reactor, to understand how performance values change as operating conditions are varied, to conduct what-if experiments, and, thereby, to assist in the design process.

The objective of this project is to simulate bed dynamics of a gas-solid fluidized bed handling fine alumina powder by applying CFD techniques. CFD modeling of fluidized beds usually adopts the Eulerian model. The focus of this experiment is on understanding the complex hydrodynamics of two-phase fluidized beds containing fine particles of micron size. The CFD software package FLUENT 13 has been used to simulate a gas - solid fluidized bed .The fluidized bed to be simulated is of height 1 m and diameter 0.05 m. The gas (air) has been injected at the base with different velocities while taking fine alumina powder of diameter 63 micron as solid bed. The static bed heights of the solid phase in the fluidized bed used for simulation are 16 cm. The 2D geometry is considered with quadrilateral meshing scheme.

5.2 CFD modeling

The model equations which are already described in literature (eq^n 2. 4 – 2. 20) are used for simulation using commercial CFD software package, FLUENT 13. The present simulation is carried out in fluidized bed of height 1 m and diameter 0.05 m. The working fluid is air and working solid is fine alumina powder having size 63 microns. Eulerian multi phase model has been used to model the transition nature of bubbling fluidized bed. The assumptions taken for simulation are no lift force, no mass transfer between gas and solid phase, constant pressure gradient and constant density of each phase. Isothermal flow condition was assumed for which there is no energy equation. Turbulent fluidization is observed with fine particles in the present work where viscosity is considered to be negligible. Thus gas phase turbulence was modeled using the k- ε model. The dispersed phases were considered as laminar. The system of equations

was solved using a finite-volume scheme; Momentum transfer between the gas and the dispersed phases was modeled using Gidaspow drag laws for the respective flow regime.

The simulation of two phase fluidized bed was performed by solving the governing equations of mass and momentum conservation using fluent software. Eulerian multi-fluid model is adopted in the present work where gas phase is treated as continuous, inter-penetrating and interacting everywhere within the computational domain. The pressure filed is assumed to be shared by all the two phases proportional to their volume fraction. The motion of each phase is governed by the respective mass and momentum equations. Two dimensional computational geometry has been generated for the fluidization column as shown in **Fig.- 5.1**. A uniform mesh i.e. Quadrilateral element structure (height to width ratio of 1) has been generated. In total, 12500 cells with size of each cell as 0.002 m x 0.002 m have been used for computation.

Initial and Boundary condition

Table 5.1 shows the initial conditions. The inlet boundary condition is designated as "velocity inlet" where the direction of gas flow is normal to the surface and the flow rate of gas is measured by different superficial gas velocity in the range of 0 to 0.067 m/s and the outlet boundary condition is the pressure boundary condition, which is set as 1.013×10^5 Pa. Wall boundary conditions are no-slip boundary conditions for the gas phase and free slip boundary conditions for the solid phase. The volume fraction of the solid is 0.9 in static bed height of the column at inlet condition.

The **phase coupled simple** method has been chosen for pressure – velocity coupling and **first order upwind scheme** has been used for discretization of volume fraction equation

whereas **second order upwind scheme** has been used for discretization of momentum, turbulent kinetic energy and turbulent dissipation rate respectively. In the discretization process; the governing partial differential equations are converted to algebraic equation. First order upwind means the value of cell at the centre is assumed to average throughout the cell and Second order upwind means a gradient is used from face cell to center cell. The initial bed of solids is packed into the bottom of the bed. The time step has been chosen as 0.001 of 1000 steps. The convergence criteria for all the numerical simulations are based on monitoring of the mass flow residual. It was observed that the residual value is converging in the range of $1.0e^{-03}$ as shown in **Fig.- 5.1**.

The relaxation factor has been used for stimulating of different flow quantities such as pressure = 0.2, density = 1, body force = 1, momentum = 0.2, volume fraction = 0.9, granular temperature = 0.2, turbulent kinetic energy = 0.5, turbulent dissipation rate = 0.5, turbulent viscosity = 1. The simulation has been carried out till the system reached quasi- steady state (flow variable is independent of time).

5.3 Study of hydrodynamic behavior

The hydrodynamics behavior of fluidized bed analyzed or the average flow variable is achieved by monitoring the expanded bed height or volume fraction of phase i.e. solid / gas phase where average value of dynamic flow characteristics is calculated in terms time, axial and radial direction. Variation of expanded bed height or volume fraction of solid phase (i.e. 63 micron alumina powder) with time for initial bed height 0.16 m at air velocity of 0.016 m/sec has been shown in **Fig. - 5.2**.

While simulating the fluidized bed, the profile of bed changes with time. But after some time no significant change in the profile is observed. This indicates that the fluidized bed has come to a Quasi – steady state. From **Fig. - 5.2**, it is observed that bed profile / expanded bed height increases up to 25 sec after that it is constant. The fully developed Quasi – steady state is reached after 30 sec. Simulation is carried out upto 60 sec (in the present case) and observed that the expanded bed height / bed profile is same in between 30 – 60 sec of simulation time (that means there is no significant change in the profile of bed).

5.3.1 Phase Dynamics

The phase dynamics of gas phase and solid phase have been represented in the form of contour plot, XY plot and vector plot. These phase dynamics are observed at air velocity 0.016 m/sec for initial bed height 0.16m of 63 micron size of alumina powder has been shown in Fig. - 5.3 to 5.6 after quasi-steady state is achieved.

From **Fig. - 5.3**, the value of volume fraction of solid phase and gas phase are calculated. The contour plot of solid i.e. alumina powder illustrates that bed is in fluidized condition. The contour plot of gas i.e. air illustrates that gas hold up is more than fluidized solid bed (i.e. volume fraction of solid is less as compared to gas) in two phase region. And also it is observed from the contour plot of air, that gas holdup is significantly more in fluidized part of the bed as compared to remaining part.

Velocity vectors

The velocity vectors for alumina powder and air in the fluidized column obtained at inlet air velocity of 0.016 m/s for static bed height of 16 cm for alumina powder of particle size 63

microns which is achieved after the quasi steady state are shown in **Fig. - 5.4**. These vectors show direction of velocity and thus help in determining flow patterns in fluidized bed

From velocity vector of solid phase (**Fig. – 5.4 (a)**), it is observed that there is vigorous movement of solid particles throughout the bed implying that the velocity at the bottom is small. It is also observed, in the middle of the bed direction of velocity near the wall downwards while that in the central region (i.e. away from wall) is upwards. At the upper part of bed i.e. fluidizing section there is circulatory motion (i.e. downward motion of the solid particles near the wall region and upward motion at central zone of the cylindrical column). No velocity vector is seen in the upper section of the column as there is no alumina powder present in this section.

The velocity vector of gas phase in the fluidized bed column is shown in **Fig. -5.4 (b)**. From **Fig.- 5.4 (b)**, It is observed that air flow is always an upward direction flow throughout the column which indicates that velocity of air is very small within the bed of particles as compared to that in remaining part of the column. This may be due to very small volume fraction of alumina powder. In the upper section of the column air velocity is high thus it carries air bubbles along with it. But in the lower section of the column solid particles obstruct the movement of bubbles thus reduces air velocity. When gas leaves fluidized part of the bed the transition from low to high velocity can be clearly seen.

XY plot:

The XY plot (**Fig. - 5.5**) show the velocity magnitude in gas phase (i.e. air) in radial direction at superficial air velocity of 0.016 m/s for initial static bed height of 0.16 m. For a fully developed flow this kind of parabolic pattern is obvious. Besides, it represents the fully

developed flow with the axial velocity being maximum at the centre line and minimum at the wall. This may be due to free slip boundary condition of gas. This plot gives a peak value of air velocity / maximum outlet velocity of air as 0.023 m/s and the minimum velocities at wall are zero.

X-Y plot is the plot of volume fraction of solid against bed height after reaching Quasi – steady state in at different simulation time. The bed height can also be calculated from XY plot of volume fraction of solid particles at air velocity of 0.016 m/sec as shown in **Fig. - 5.6**. Bed height is determined by taking volume fraction of solid i.e. alumina powder on Y-axis while height of the bed on X-axis in 2D mesh.

From **Fig. – 5.6**, it is observed that solid volume fraction (i.e. alumina powder) increases in axial direction with minimum value at bottom of bed / base of the column. When steady state is attained gas hold up remains constant (after 30 sec). A point is reached where the solid volume fraction sharply decreases to zero is the indication of the maximum fluidization. From this maximum expanded bed height is obtained.

5.4 Bed expansion

Fig. -5.7 shows a set of contours of solid volume fraction of 63 microns alumina powder at inlet air velocity of 0.016 m/sec for initial bed height of 16 cm. It is observed that the expanded bed height / bed profile increases in gas – solid system with increase in gas/air velocity and simultaneously bed voidage increases / solid volume fraction decreases. Experimentally the same trend is also observed.

<u>XY plot:</u>

The bed height of the column is calculated in terms of volume fraction of solid. It is observed that the bed height increases with increase of air velocity as shown in **Fig. 5.8**. The bed height of alumina powder is represented in XY plot (**Fig. – 5. 8**).

A comparison of experimental and simulated results for expansion ratio at different air velocities at bed height 16 cm has been shown in **Fig. -5.9**. It is found that simulated results are in good agreement with experimental results with a 28% deviation (approx.).

Experimentally, the expanded bed height / bed profile has been calculated by varying particle density, particle size in cylindrical column. A comparison has been made with CFD simulation. **Fig.- 5.10** represents contour plot of volume fraction of solid at constant air velocity of 0.016 m/sec for initial bed height 0.16 m in cylindrical column. It is observed that with increase in particle size and density of particle, the solid volume fraction decreases i.e. expanded bed height increases.

The bed expansion is clearly studied from X-Y plot i.e. volume fraction of solid against different densities of static bed height 16 cm as shown in **Fig.- 5.11.** Bed height is determined by taking volume fraction of fine solid particles along Y-axis while density of solid is taken along X-axis after reaching Quasi – steady state. From **Fig. -5.11**, it is observed that the volume fraction of solid particles decreases with increase in particle size and density. That means the bed expansion decreases with increase of particle density / particle size.

A comparison of experimental and simulated results obtained at constant air velocity of 0.016 m/s and initial bed height 16 cm for different density of particle has been shown in **Fig. – 5.12**. It is observed that as density increases, solid volume fraction increases upto certain level and then decreases and understood that simulated results are in good agreement with experimental results with a 32% deviation (approx.).

CFD simulation of hydrodynamics of gas- solid fluidized bed has been carried out for different operating condition by employing the Eulerian – Eulerian granular multi-phase approach. The CFD simulation results have shown good agreement with experimental data for solid phase hydrodynamics in terms of expanded bed height. The bed expansion height increases with gas velocity and decreases with particle size as well as particle density. Experimental result and CFD analysis have shown an increase in bed expansion with gas velocity and particle density.

Table – 5.1: Initial Condition of CFD Simulation for Column of ID 0.05 m and Height 1 m

(a) <u>Solid phase:-</u>

Sample	Magnetite	Talcum powder	Silicon Carbide	Alumina
Particle size	$75*10^{-6}$ m	$80*10^{-6}$ m	$70*10^{-6}$ m	$63*10^{-6}$ m
Particle density	2400 kg/m^3	880 kg/m^3	720 kg/m^3	640 kg/m^3
Initial static bed height	0.016 m	0.016 m	0.016 m	0.016 m
Static bed voidage	0.9	0.9	0.9	0.9

(b) <u>Gas Phase :-</u>

Sample	Air
Viscosity	$1.8 *10^{-5}$ Pa s
Density	1.17 kg / m^3
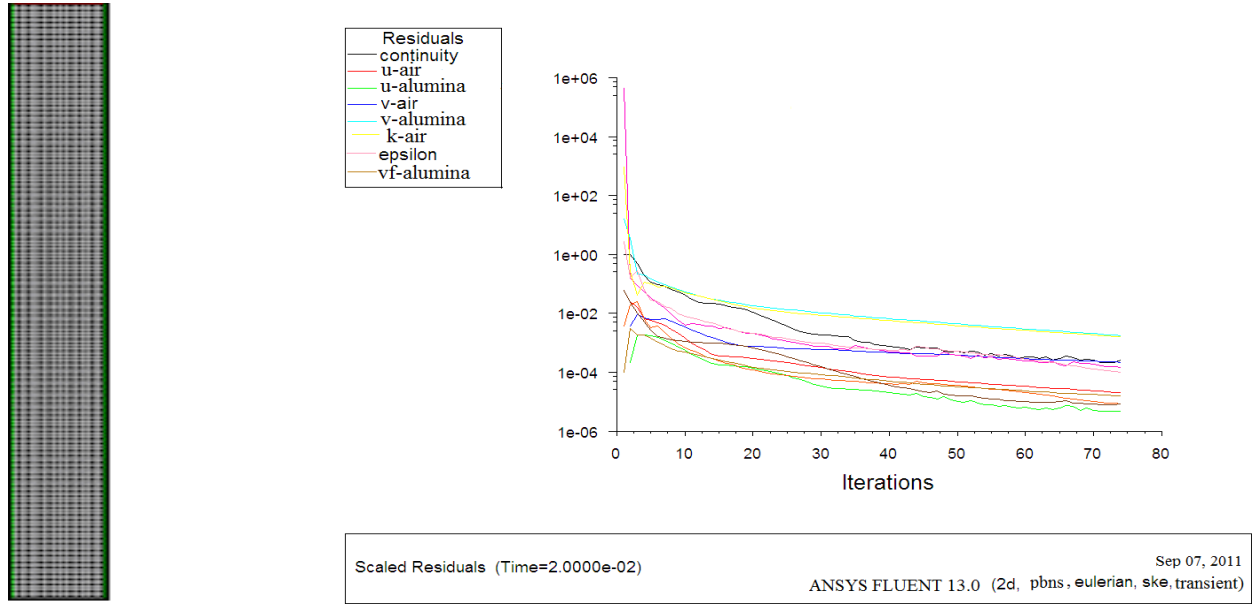
| 2 D Mesh | Plot of residuals with the progress of simulation |

Figure -5.1: Mesh and Residual Plot of Simulation

0sec   5sec   10sec   15sec   20sec   25sec   30sec   35sec   40sec   45 sec   50sec   55sec 60sec
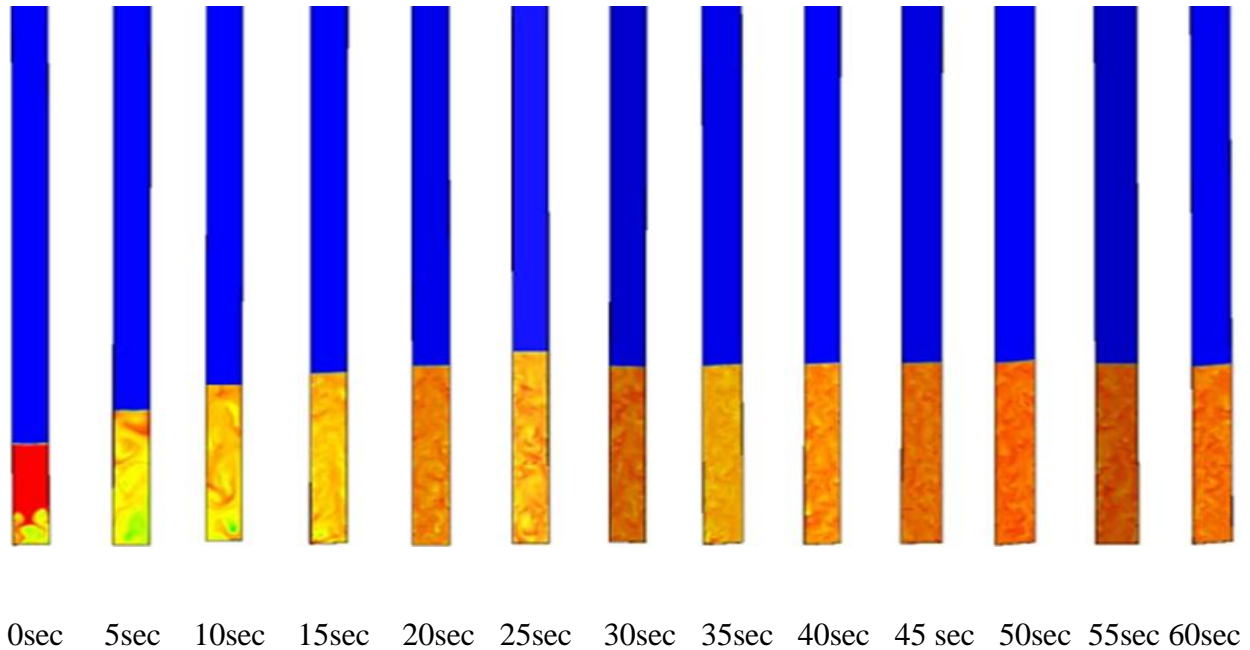
Figure -5.2: Contour Plot of Volume Fraction for Alumina Powder m/sec with respect of

Time
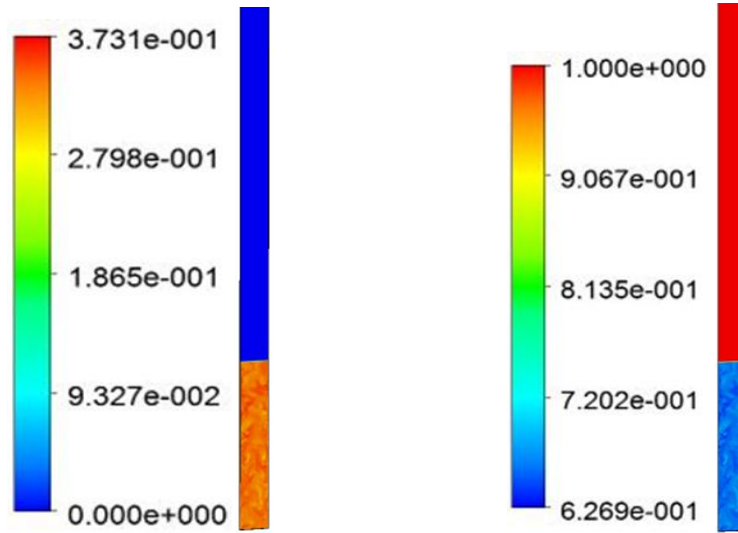
Solid Phase   Gas Phase

Figure -5.3: Contour Plot of Volume Fraction of Solid Phase and Gas Phase
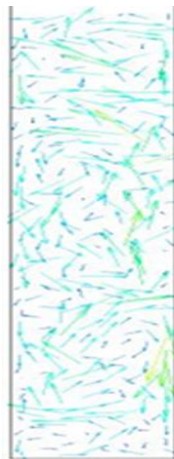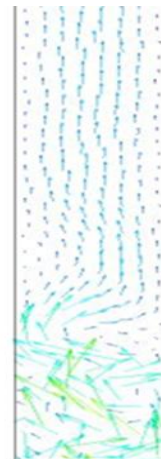
(a) Solid phase   (b) Gas phase

Figure -5.4: Velocity Vector Solid phase and Gas phase
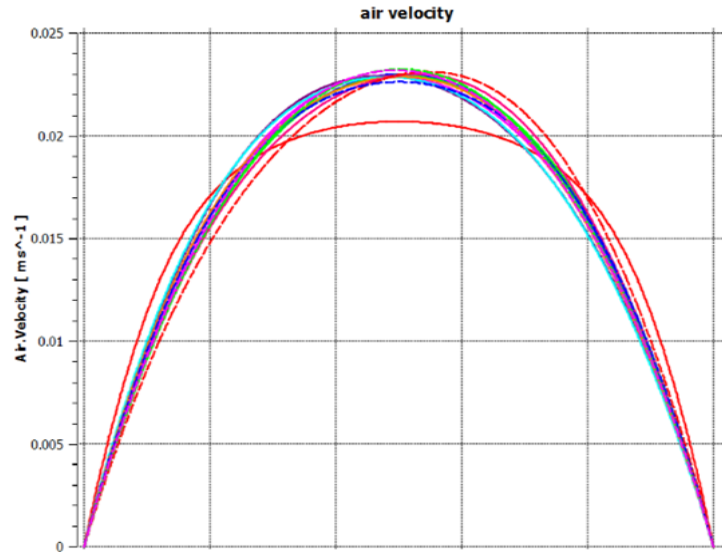
Figure -5.5: XY Plot of Velocity Magnitude in Gas Phase
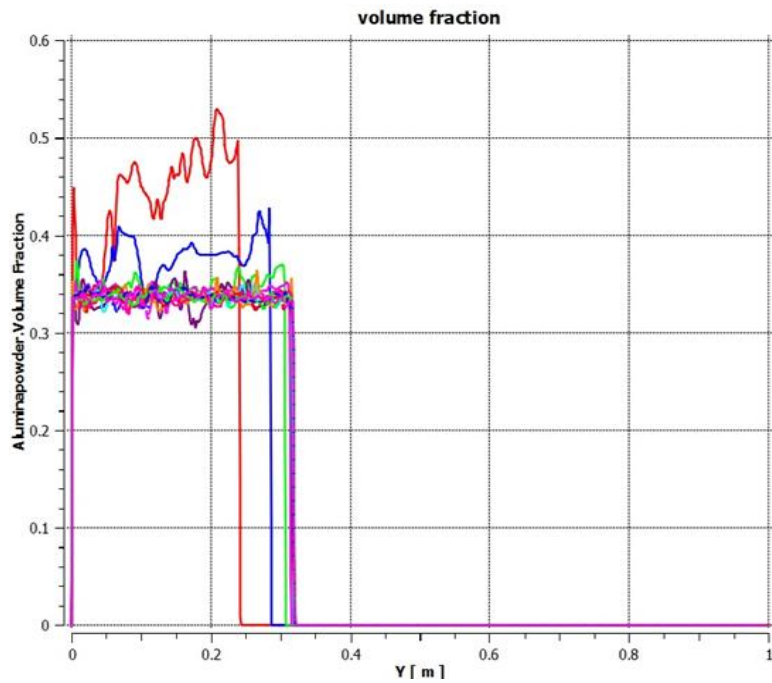
Figure -5.6: XY Plot of Solid Volume Fraction
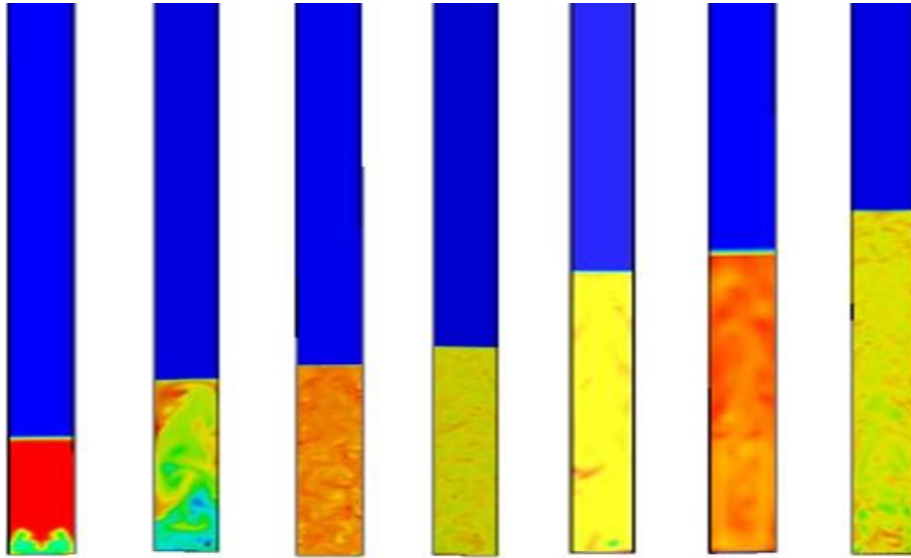
0.016 m/s   0.021 m/s   0.033 m/s   0.038 m/s 0.046m/s   0.059 m/s   0.067m/s

Figure –5.7: Contour plot of Solid Volume Fraction of Alumina Powder at Different Air Velocities
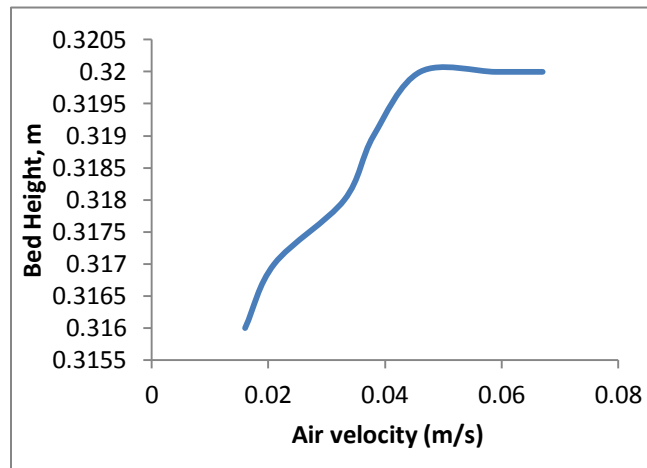
Figure - 5.8: XY plot of Bed Height against Air Velocity
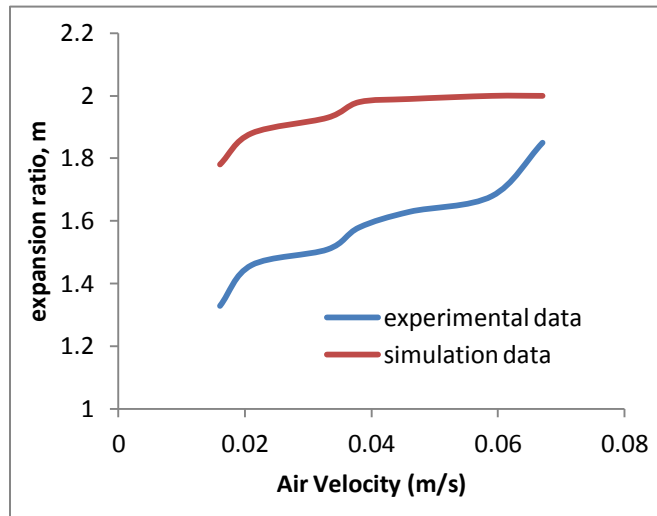
Figure – 5.9: Comparison of Experimental and Simulated Results for Expansion Ratio at Different Air Velocities

Magnetite   Silicon Carbide   Alumina Powder   Talcum Powder
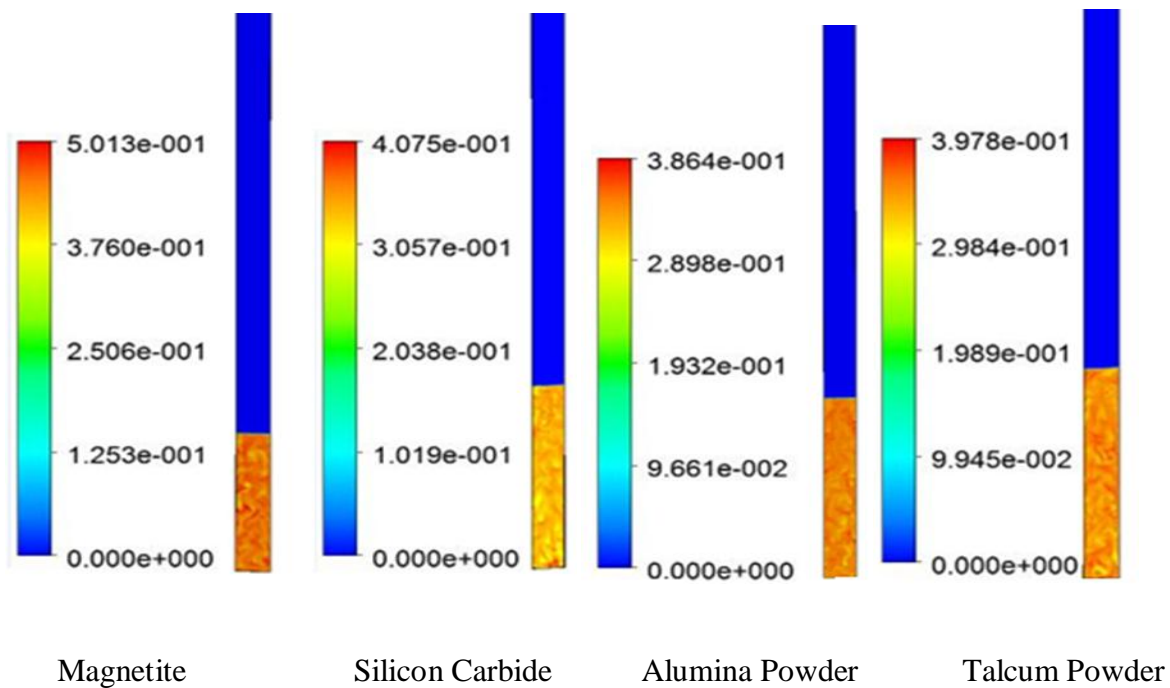
Figure – 5.10: Contour plot of Volume Fraction of Solid Materials at different particle densities
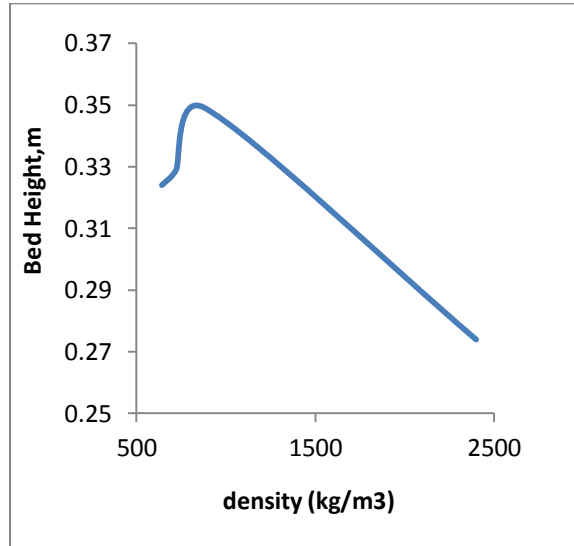
Figure -5.11: XY plot of Bed Height against Density of Solids
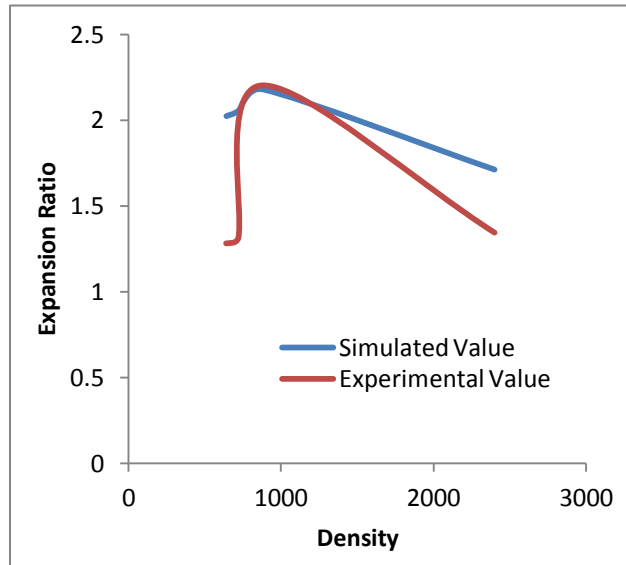
Figure – 5.12: Comparison of Experimental and Simulated Results for Expansion Ratio at Different Densities

CHAPTER - 6

RESULTS AND DISCUSSION

RESULTS AND DISCUSSION

6.1 CORRELATION PLOTS

Correlations have been developed for the bed expansion / fluctuation ratio, fluidization Index by varying different system parameters on the basis of dimensionless analysis. Dimensionless analysis helps one understand how the typical value of the dependent variable i.e. bed expansion ratio, bed fluctuation ratio, fluidization Index changes when any one of the independent variables is varied, while the other independent variables are held fixed. The calculated values of these bed dynamics thus obtained through correlation equations have been compared with the experimentally observed values. These developed correlations are obtained through eq^n- 2.1, 2.2 and 2.3.

The applicability of correlation plots are:

- The effect of parameters can be known, for designing the process equipment and optimizing the process.

- These correlations give the base of the design for the industrial equipments.

- These correlations can be used directly in the laboratory scale.

- These correlations need to be scaled up for pilot plant unit and industrial equipment.

6.1.1 Correlation Plots for Coarse (Regular / Irregular) particles

The correlation plots of bed expansion / fluctuation ratio and fluidization index for coarse (regular / irregular) particles in spouted bed are shown in **Fig. - 6.1, 6.2 and 6.3**. The observed and calculated values of these bed dynamics have been compared in **Table – 6.1 and 6.2** for coarse regular and irregular particles respectively in spouted bed. The comparison of standard

and mean deviations of coarse regular and irregular particles in spouted bed are listed in Table – 6.3.

6.1.1.1 Bed Expansion Ratio

The correlations developed for bed expansion ratio on the basis of dimensionless analysis are as follows

(i)   For Regular Coarse Particle

$$R = 0.0271 \left(\frac{H_s}{D_c}\right)^{-0.009} \left(\frac{\rho_s}{\rho_f}\right)^{0.364} \left(\frac{d_p}{D_c}\right)^{0.4} \left(\frac{D_i}{D_c}\right)^{-0.3} \left(\frac{U_0}{U_{mf}}\right)^{0.09} \tag{6.1}$$

(ii)   For Irregular Coarse Particle

$$R = 1.1707 \left(\frac{H_s}{D_c}\right)^{-0.027} \left(\frac{\rho_s}{\rho_f}\right)^{0.001} \left(\frac{d_p}{D_c}\right)^{0.112} \left(\frac{D_i}{D_c}\right)^{-0.052} \left(\frac{U_0}{U_{mf}}\right)^{2.11} \tag{6.2}$$

6.1.1.2 Bed Fluctuation Ratio

The correlations developed for bed fluctuation ratio on the basis of dimensionless analysis are as follows

(i)   For Regular Coarse Particles

$$r = 0.006 \left(\frac{H_s}{D_c}\right)^{-0.08} \left(\frac{\rho_s}{\rho_f}\right)^{0.44} \left(\frac{d_p}{D_c}\right)^{-0.69} \left(\frac{D_i}{D_c}\right)^{0.38} \left(\frac{U_0}{U_{mf}}\right)^{0.2} \tag{6.3}$$

(ii)   For Irregular Coarse Particles

$$r = 1.648 \left(\frac{H_s}{D_c}\right)^{-0.05} \left(\frac{\rho_s}{\rho_f}\right)^{0.002} \left(\frac{d_p}{D_c}\right)^{0.206} \left(\frac{D_i}{D_c}\right)^{-0.001} \left(\frac{U_0}{U_{mf}}\right)^{2.99} \tag{6.4}$$

6.1.1.3 Fluidization Index

The correlations developed for fluidization index of coarse particles on the basis of dimensionless analysis are as follows

(i)   For Regular Coarse Particle

$$FI= 0.0313 \left(\frac{H_s}{D_c}\right)^{-0.084} \left(\frac{\rho_s}{\rho_f}\right)^{0.528} \left(\frac{d_p}{D_c}\right)^{0.646} \left(\frac{D_i}{D_c}\right)^{-0.628} \left(\frac{U_0}{U_{mf}}\right)^{0.463} \qquad (6.5)$$

(ii)   For Irregular Coarse Particle

$$FI= 0.0096 \left(\frac{H_s}{D_c}\right)^{-0.155} \left(\frac{\rho_s}{\rho_f}\right)^{0.521} \left(\frac{d_p}{D_c}\right)^{-0.354} \left(\frac{D_i}{D_c}\right)^{0.321} \left(\frac{U_0}{U_{mf}}\right)^{-0.189} \qquad (6.6)$$

6.2 Correlation plot for Fine particles in Fluidized / Spouted bed:

The correlation plots of bed expansion / fluctuation ratio and fluidization index for fine particles in fluidized / spouted bed are shown in **Fig. - 6.4, 6.5 and 6.6**. The observed and calculated values of these bed dynamics have been compared in **Table – 6.4 and 6.5** for fine particles in fluidized bed and spouted bed respectively. The comparison of standard and mean deviations of fine particles in fluidized / spouted bed are listed in **Table – 6.6**.

6.2.1 Bed expansion ratio

The correlations developed for bed expansion ratio in fluidized / spouted bed of fine particles on the basis of dimensionless analysis are as follows

(i)   In fluidized bed

$$R= 0.006 \left(\frac{H_s}{D_c}\right)^{-0.003} \left(\frac{\rho_s}{\rho_f}\right)^{0.123} \left(\frac{d_p}{D_c}\right)^{0.63} \left(\frac{U_0}{U_{mf}}\right)^{0.72} (N)^{-0.007} \qquad (6.7)$$

(ii)   In spouted bed

$$R = 0.838 \left(\frac{H_s}{D_c}\right)^{-0.01} \left(\frac{\rho_s}{\rho_f}\right)^{0.021} \left(\frac{d_p}{D_c}\right)^{-0.009} \left(\frac{D_i}{D_c}\right)^{-0.008} \left(\frac{U_0}{U_{mf}}\right)^{0.609} \qquad (6.8)$$

6.2.2 Bed fluctuation ratio

The correlations developed for bed fluctuation ratio in fluidized / spouted bed of fine particles on the basis of dimensionless analysis are as follows

(i)   In fluidized bed

$$r = 0.05 \left(\frac{H_s}{D_c}\right)^{-0.003} \left(\frac{\rho_s}{\rho_f}\right)^{0.079} \left(\frac{d_p}{D_c}\right)^{-0.40} \left(\frac{U_0}{U_{mf}}\right)^{0.22} (N)^{-0.009} \qquad (6.9)$$

(ii)   In spouted bed

$$r = 0.674 \left(\frac{H_s}{D_c}\right)^{-0.036} \left(\frac{\rho_s}{\rho_f}\right)^{0.043} \left(\frac{d_p}{D_c}\right)^{-0.019} \left(\frac{D_i}{D_c}\right)^{-0.031} \left(\frac{U_0}{U_{mf}}\right)^{0.412} \qquad (6.10)$$

6.2.3 Fluidization Index

The correlations developed for fluidization index in fluidized / spouted bed of fine particles on the basis of dimensionless analysis are as follows

(i)   In fluidized bed

$$FI = 0.075 \left(\frac{H_s}{D_c}\right)^{-0.161} \left(\frac{\rho_s}{\rho_f}\right)^{0.11} \left(\frac{d_p}{D_c}\right)^{-0.041} \left(\frac{U_0}{U_{mf}}\right)^{-0.48} (N)^{0.159} \qquad (6.11)$$

(ii)   In spouted bed

$$FI = 168.69 \left(\frac{H_s}{D_c}\right)^{-0.06} \left(\frac{\rho_s}{\rho_f}\right)^{-0.45} \left(\frac{d_p}{D_c}\right)^{0.46} \left(\frac{D_i}{D_c}\right)^{-0.08} \left(\frac{U_0}{U_{mf}}\right)^{-0.36} \qquad (6.12)$$

6.3 Discussion for Correlation Plots

It was observed that increase of spout diameter decreases the bed expansion/ fluctuation ratio and fluidization index because of more amount of air passing in the central region only in case of spouted bed. In case of fluidized bed the increased speed of rotation of stirrer and increased frequency of application of external force breaks the bubbles and agglomerations of fine particles thereby reducing the bed expansion / fluctuation ratio and fluidization index. The high value of the correlation coefficient for coarse, fine particles in both fluidized / spouted bed indicates that the dimensionless analysis explains well the variations of dependent variable. The calculated values of the bed expansion / fluctuation ratio, fluidization index obtained through dimensionless analysis are compared with the experimentally observed values. The deviations of calculated values are found to be within +15% to -15% and mean deviation within 1 to 7% for coarse and   -1 to 5% for fine particles.

6.4 Nano Fluidization

The effects of the different system parameters on hydrodynamic behaviors of copper nano materials (i.e. $d_p = 70$ nm and surface area= $5 m^2/gm$) have been studied in the present work.

6.4.1 Effects of Velocity

Effect of superficial velocity on bed dynamics has been studied (**Fig.-6.7**) for different static bed heights at constant external force.

6.4.2 Effect of External Force

During the fluidization process for nano particles, it was observed that all the materials are lifted up as a single mass and then disintegrated to form stable channels. The bed expands

slightly with an uneven surface (as slugging phenomenon takes place). On application of external force, the bed collapses in a few of seconds, the channels then disappear and the bed expands rapidly and uniformly until it reaches the full expansion. A homogenous fluidization state is then easily established.

The external force can be calculated as follows:

External Force = Centrifugal Force $F = m * a = m * r\omega^2$ (6.13)

Effects of external force on bed dynamics i.e. bed pressure drops, bed expansion ratio, bed fluctuation ratio and fluidization index of copper nano materials at constant static bed height as well as superficial velocity are shown in **Fig. – 6.8**.

6.4.3 Discussion for Nano Fluidization

The variation of bed pressure drop against the superficial gas velocity was plotted for each set of experiment from which the minimum fluidization velocities for nano particles were observed. A sample plot is shown in **Fig. -6.7 (a) and 6.8 (a)**. It is observed that the bed pressure drop gradually increases with increase in velocity up to certain limit after which it remains constant once true fluidization is attained.

It is observed that with the increase in superficial velocity (U_o) both the expansion and fluctuation ratio increases monotonically in fluidized bed in **Fig.- 6.7 (b), (c) and 6.8 (b), (c)**, indicating that more bubbles forms as superficial velocity exceeds minimum fluidization velocity. As a result bed expands. As bubble size increases further with increase in superficial velocity of fluid, bed expansion as well as bed fluctuation ratio increase.

Fluidization index values were found out to be approximately 1 indicating the case of ideal fluidization. This implies that the application of the external force results in proper fluidization in **Fig. – 6.7 (d) and 6.8 (d)**.

Comparison of variation in bed dynamics with superficial velocity of fluid for different static bed height as shown in **Fig. - 6.7** at constant external force i.e. 4.2 N. It is observed that, bed expansion / fluctuation ratio and fluidization index decrease as increase of static bed height. The bed pressure drops increases with increase in static bed height.

As nano particles exhibit only slugging and channeling even at low gas velocities in a fluidized bed. With the application of external force, the bed of nano particles fluidize smoothly. With the aid of external force to the column, large agglomerate clusters break down due to combined effect of hydrodynamic force and external force. The pressure drop increases with increase of static bed height while other parameters constant.

The bed expansion / fluctuation ratio were also observed to increase linearly due to large bed voidage and lighter weight of nano particles. In case of low static bed height, bed materials might be entrained and expanded bed height might not be properly observed. Application of external force, reduces bed expansion / fluctuation ratio and improves fluidization index with increase of static bed height while other parameters remains constant.

Attempt was made to compare the effects of different amounts of external forces on bed dynamics by varying the superficial velocity of fluid as shown in **Fig. –6.8** at constant static bed height i.e. 8 cm. From Fig.-6.8, it is observed that increased external force decreases substantially all the bed dynamics under investigation i.e. bed pressure drop (ΔP), bed expansion ratio (R), fluctuation ratio (r) and fluidization index (F.I.). As increased external force reduces all

the bed dynamics substantially minimum fluidization velocity also decreases and also frequent breaking of air bubbles. So that it prevents entrainment and elutriation of particles.

Table – 6.1: Observed Data and Calculated Values of Bed Dynamics for Spouting Process of Coarse Regular Particles

Sl. No	H_s/D_c	ρ_s/ρ_f	d_p/D_c	D_i/D_c	U_o/U_{mf}	R		r		F.I.	
						R_{exp}	R_{cal}	r_{exp}	r_{cal}	F.I. $_{exp}$	F.I. $_{cal}$
1	0.8	2211.809	0.033	0.25	1	1.181	1.166	1.223	1.214	0.606	0.672
2	1.2	2211.809	0.033	0.25	1	1.112	1.161	1.119	1.172	0.674	0.675
3	1.6	2211.809	0.033	0.25	1	1.09	1.158	1.102	1.144	0.642	0.677
4	2	2211.809	0.033	0.25	1	1.182	1.155	1.14	1.122	0.931	0.678
5	0.8	2530.459	0.033	0.25	1	1.237	1.224	1.162	1.289	0.805	0.666
6	0.8	1030.928	0.033	0.25	1	1	0.882	1	0.862	0.821	0.706
7	0.8	1255.858	0.033	0.25	1	1	0.948	1	0.942	0.513	0.697
8	0.8	2211.809	0.026	0.25	1	1.381	1.282	1.569	1.43	0.812	0.685
9	0.8	2211.809	0.022	0.25	1	1.712	1.371	2.078	1.605	0.539	0.694
10	0.8	2211.809	0.017	0.25	1	1.506	1.52	1.802	1.916	0.791	0.708
11	0.8	2211.809	0.033	0.3	1	1.275	1.232	1.428	1.301	0.799	0.681
12	0.8	2211.809	0.033	0.35	1	1.293	1.29	1.379	1.38	0.704	0.689
13	0.8	2211.809	0.033	0.4	1	1.381	1.343	1.483	1.452	0.733	0.697
14	0.8	2211.809	0.033	0.25	1.1	1.006	1.161	1.012	1.203	0.606	0.674
15	0.8	2211.809	0.033	0.25	1.2	1.006	1.17	1.012	1.225	0.606	0.670
16	0.8	2211.809	0.033	0.25	1.3	1.018	1.175	1.037	1.235	0.606	0.668

Table – 6.2: Observed Data and Calculated Values of Bed Dynamics for Spouting Process of Coarse Irregular Particles

Sl.No	H_s/D_c	ρ_s/ρ_f	d_p/D_c	D_i/D_c	U_o/U_{mf}	R		r		F.I.	
						R_{exp}	R_{cal}	r_{exp}	r_{cal}	$F.I._{exp}$	$F.I._{cal}$
1	0.8	2282.6	0.033	0.25	1	1.031	0.868	1.062	1.021	0.945	0.97
2	1.2	2282.6	0.033	0.25	1	1.004	0.861	1.008	0.999	1.033	0.917
3	1.6	2282.6	0.033	0.25	1	1.015	0.856	1.031	0.983	0.577	0.881
4	2	2282.6	0.033	0.25	1	1.002	0.852	1.005	0.971	0.857	0.855
5	0.8	1513.3	0.033	0.25	1	1.018	0.868	1.062	1.02	1.31	0.794
6	0.8	1236.2	0.033	0.25	1	1.006	0.868	1.008	1.019	0.974	0.719
7	0.8	655.9	0.033	0.25	1	1.012	0.867	1.031	1.018	0.425	0.528
8	0.8	2282.6	0.026	0.25	1	1.25	0.845	1.5	0.971	0.867	1.036
9	0.8	2282.6	0.022	0.25	1	1.012	0.83	1.025	0.938	1.112	1.085
10	0.8	2282.6	0.017	0.25	1	1.012	0.806	1.025	0.888	1.44	1.165
11	0.8	2282.6	0.033	0.3	1	1.006	0.86	1.0125	1.02	0.84	1.035
12	0.8	2282.6	0.033	0.35	1	1.006	0.853	1.012	1.02	1.307	1.093
13	0.8	2282.6	0.033	0.4	1	1.006	0.847	1.012	1.02	1.138	1.146
14	0.8	2282.6	0.033	0.25	1.1	1.175	1.022	1.136	0.886	1.44	0.976
15	0.8	2282.6	0.033	0.25	1.2	1.375	1.187	1.444	1.168	1.364	0.964
16	0.8	2282.6	0.033	0.25	1.3	1.531	1.361	1.578	1.329	1.364	0.958

Table - 6.3: Comparison Results of Bed Dynamics for Coarse Particle in Spouted Bed

Items	R		r		FI	
	Regular	Irregular	Regular	Irregular	Regular	Irregular
Standard Deviation	-11 - +7 %	-5 - +10 %	-13 - +8 %	-2 - +15 %	-10 - +15%	-18% to +11%
Mean Deviation	1.05 %	6.07 %	3.95 %	3.79 %	4.62 %	1.28 %

Table – 6.4: Observed Data and Calculated Values of Bed Dynamics for Fluidization Process of Fine Particles

Sl.No	H_s/D_c	ρ_s/ρ_f	d_p/D_c	U_o/U_{mf}	N	R		r		F.I.	
						R_{exp}	R_{cal}	r_{exp}	r_{cal}	$F.I._{exp}$	$F.I._{cal}$
1	3.2	692.91	0.0013	1.25	121.2	1.031	1.062	1.062	1.008	0.749	0.786
2	4.4	692.91	0.0013	1.25	121.2	1.045	1.061	1.09	1.029	0.772	0.763
3	5	692.91	0.0013	1.25	121.2	1.02	1.06	1.04	1.025	0.755	0.754
4	5.6	692.91	0.0013	1.25	121.2	1.035	1.06	1.071	1.021	0.89	0.746
5	3.2	503.93	0.0013	1.25	121.2	1.031	1.021	1.062	1.015	0.942	0.802
6	3.2	566.92	0.0013	1.25	121.2	1.031	1.036	1.062	1.024	0.958	0.796
7	3.2	1889.76	0.0013	1.25	121.2	1.187	1.203	1.235	1.123	0.805	0.737
8	3.2	692.91	0.0012	1.25	121.2	1.187	1.117	1.235	1.072	0.845	0.788
9	3.2	692.91	0.0014	1.25	121.2	1.031	1.013	1.062	1.011	0.958	0.785
10	3.2	692.91	0.0015	1.25	121.2	1.031	0.97	1.062	0.984	0.942	0.783
11	3.2	692.91	0.0013	1.5	121.2	1.187	1.212	1.054	1.081	0.642	0.746
12	3.2	692.91	0.0013	1.75	121.2	1.375	1.356	1.135	1.117	0.642	0.714
13	3.2	692.91	0.0013	2	121.2	1.5	1.494	1.2	1.149	0.642	0.688
14	3.2	692.91	0.0013	1.25	73.9	1.031	1.066	1.062	1.043	0.712	0.648
15	3.2	692.91	0.0013	1.25	101.6	1.031	1.063	1.062	1.041	0.811	0.734
16	3.2	692.91	0.0013	1.25	137.4	1.512	1.061	1.05	1.039	0.942	0.826

Table – 6.5: Observed Data and Calculated Values of Bed Dynamics for Spouting Process of Fine Particles

Sl.No	H_s/D_c	ρ_s/ρ_f	d_p/D_c	D_i/D_c	U_o/U_{mf}	R		r		F.I.	
						R_{exp}	R_{cal}	r_{exp}	r_{cal}	$F.I._{exp}$	$F.I._{cal}$
1	1.6	677.16	0.00126	0.06	1	1.031	1.034	1.062	1.076	0.801	0.974
2	2.4	677.16	0.00126	0.06	1	1.083	1.026	1.166	1.06	0.655	0.949
3	3.2	677.16	0.00126	0.06	1	1.015	1.021	1.031	1.049	0.754	0.932
4	4	677.16	0.00126	0.06	1	1.025	1.018	1.05	1.04	0.722	0.919
5	1.6	503.93	0.00126	0.06	1	1.031	1.027	1.062	1.062	1.328	1.08
6	1.6	1173.2	0.00126	0.06	1	1.062	1.046	1.125	1.102	0.618	0.803
7	1.6	1259.8	0.00126	0.06	1	1.043	1.047	1.087	1.105	0.899	0.783
8	1.6	677.16	0.0009	0.06	1	1.031	1.036	1.037	1.062	0.819	0.834
9	1.6	677.16	0.0018	0.06	1	1.031	1.03	1.062	1.069	0.848	1.147
10	1.6	677.16	0.0025	0.06	1	1.018	1.028	1.062	1.082	1.456	1.334
11	1.6	677.16	0.00126	0.02	1	1.043	1.043	1.087	1.109	0.78	1.064
12	1.6	677.16	0.00126	0.04	1	1.062	1.037	1.125	1.088	1.281	1.006
13	1.6	677.16	0.00126	0.08	1	1.018	1.031	1.037	1.067	0.86	0.951
14	1.6	677.16	0.00126	0.06	1.25	1.062	1.186	1.125	1.179	0.801	0.893
15	1.6	677.16	0.00126	0.06	1.5	1.343	1.327	1.388	1.271	0.801	0.832
16	1.6	677.16	0.00126	0.06	1.75	1.512	1.459	1.304	1.355	0.801	0.784

Table - 6.6: Comparison results for Bed Dynamics of fine Particles in fluidized/Spouted Bed

Items	R		r		F. I.	
	Fluidized Bed	Spouted Bed	Fluidized Bed	Spouted Bed	Fluidized Bed	Spouted Bed
Standard Deviation	- 4 - +5 %	-11 - +5 %	-2 - +13 %	- 4 - +9 %	-11 - +16 %	-18 - +11%
Mean Deviation	- 0.578 %	- 0.047 %	4.15 %	0.019 %	5.008 %	- 0.055 %

Regular Particles

$y = 0.0271x^{0.977}$

Rexp

30

0.8

$(H_s/D_c)^{-0.01} (\rho_s/\rho_f)^{0.373} (d_p/D_c)^{0.415} (D_i/D_c)^{-0.309} (U_o/U_{mf})^{0.09}$

Irregular Particles

10

$1.1707x^{1.0745}$

Rexp

0.5

1

$(H_s/D_c)^{-0.026} (\rho_s/\rho_f)^{0.001} (d_p/D_c)^{0.105} (D_i/D_c)^{-0.049} (U_0/U_{mf})^{1.97}$

Figure - 6.1: Correlation Plots of Bed Expansion Ratio against System Parameters for

Coarse Particles

Regular Particles

$y = 0.006x^{1.0754}$

rexp

80

0.6

$(H_s/D_c)^{-0.085} (\rho_s/\rho_f)^{0.417} (d_p/D_c)^{-0.641} (D_i/D_c)^{0.354} (U_0/U_mf)^{0.188}$

Irregular Particles

$y = 1.6485x^{1.0631}$

r exp

0.5

0.5

$(H_s/D_c)^{-0.026} (\rho_s/\rho_f)^{0.001} (d_p/D_c)^{0.105} (D_i/D_c)^{-0.049} (U_0/U_{mf})^{1.97}$

Figure - 6.2: Correlation Plot of Bed Fluctuation Ratio against System Parameters for

Coarse Particles

Regular Particles

$y = 0.0313x^{1.2}$

$(H_s/D_c)^{-0.07} (\rho_s/\rho_f)^{0.44} (d_p/D_c)^{0.539} (D_i/D_c)^{-0.524} (U_0/U_{mf})^{0.386}$

F.I. exp

Irregular Particles

$y = 0.0096x^{0.5111}$

$(H_s/d_c)^{-0.3} (\rho_s/\rho_f)^{1.02} (d_p/D_c)^{-0.6} (D_i/D_c)^{0.63} (U_o/U_{mf})^{-0.371}$

FI exp

Figure - 6.3: Correlation Plot of Fluidization Index against System Parameters for Coarse Particles

Fluidization Process

$y = 0.0061x^{1.0892}$

$(H_s/D_c)^{-0.003} (\rho_s/\rho_f)^{0.114} (d_p/D_c)^{-0.584} (U_0/U_{mf})^{0.677} (N)^{-0.007}$

Rexp

Spouting Process

$y = 0.8381x^{0.846}$

$(H_s/D_c)^{-0.022} (\rho_s/\rho_f)^{0.025} (d_p/D_c)^{-0.011} (D_i/D_c)^{-0.01} (U_0/U_{mf})^{0.72}$
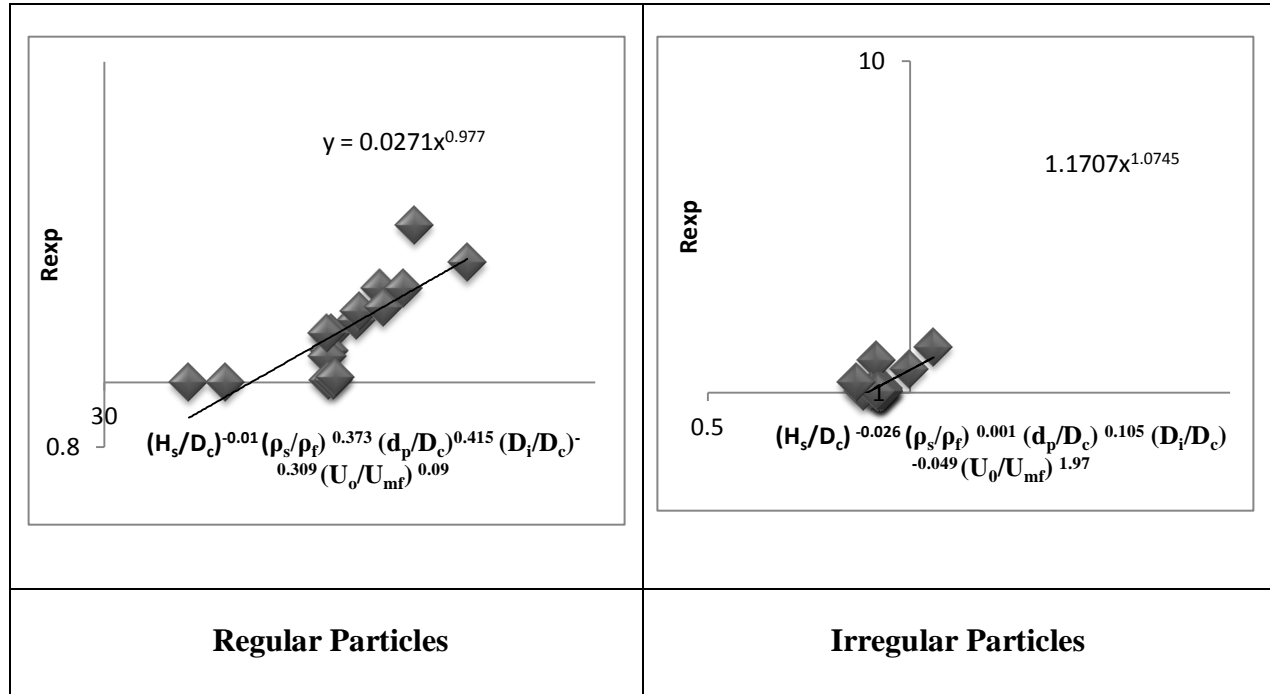
R exp

Figure - 6.4: Correlation Plot of Bed Expansion Ratio against System Parameters for Fine Particles
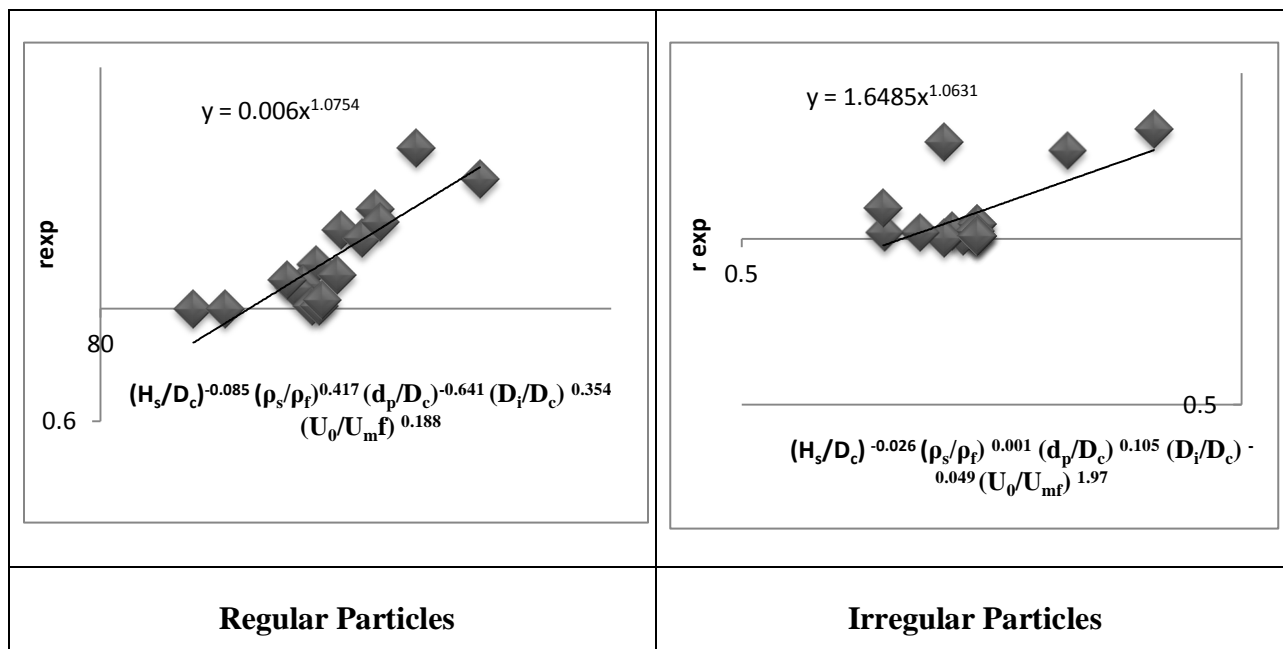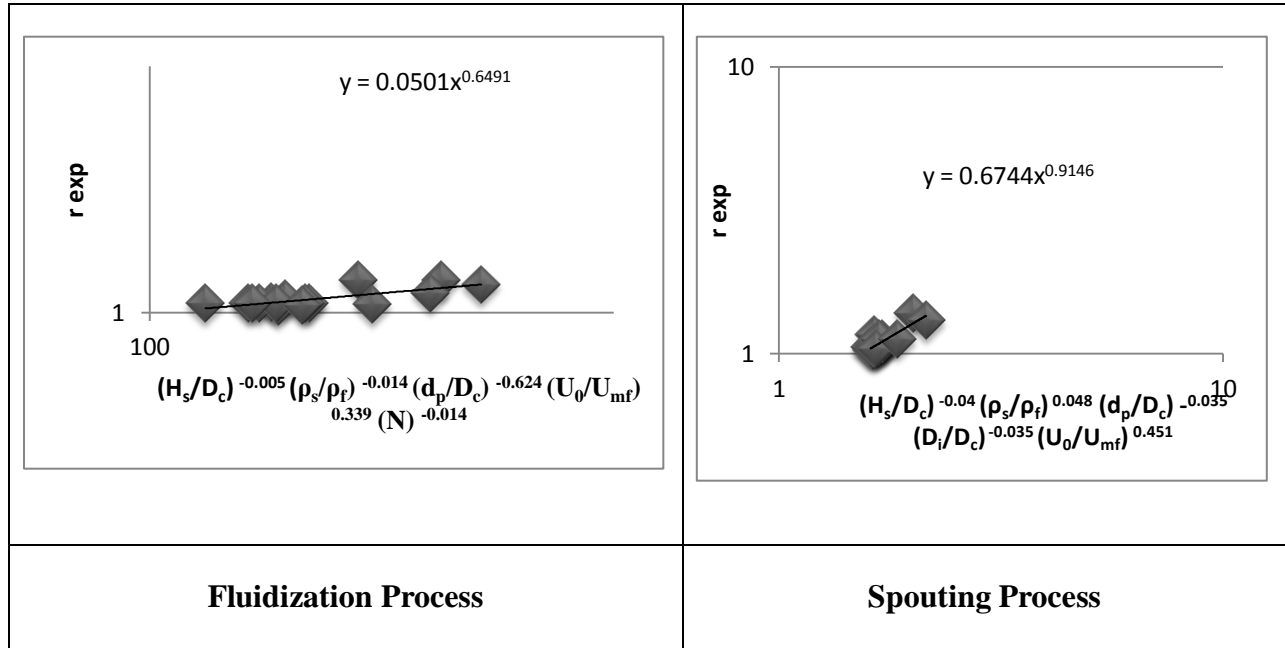
Figure - 6.5: Correlation Plot of Bed Fluctuation Ratio against System Parameters for Fine Particles
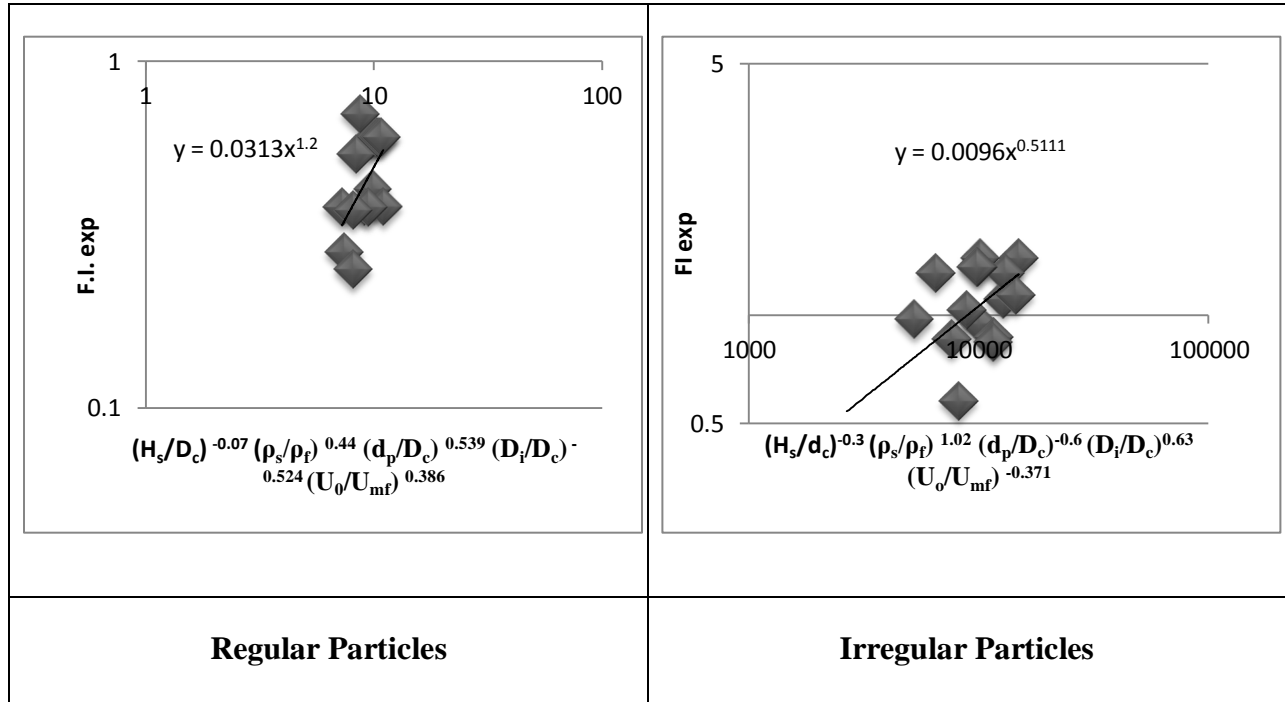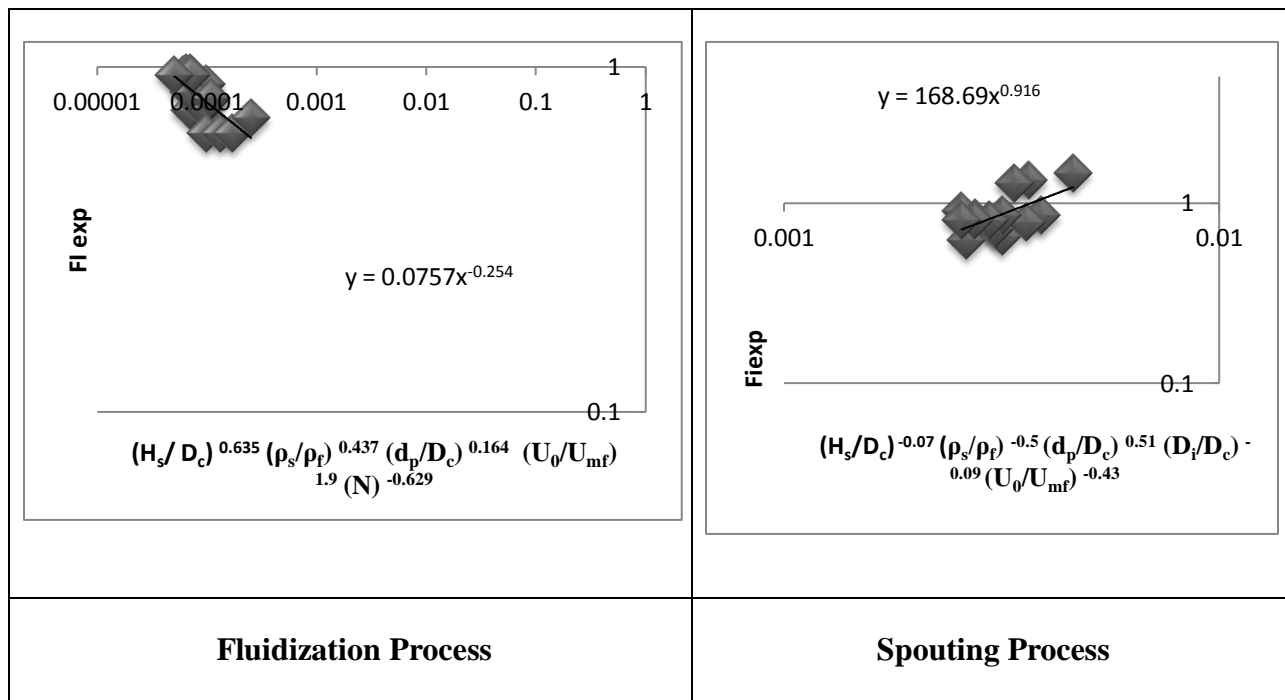

Figure - 6.6: Correlation Plot of Bed Fluidization Index against System Parameters for Fine Particles
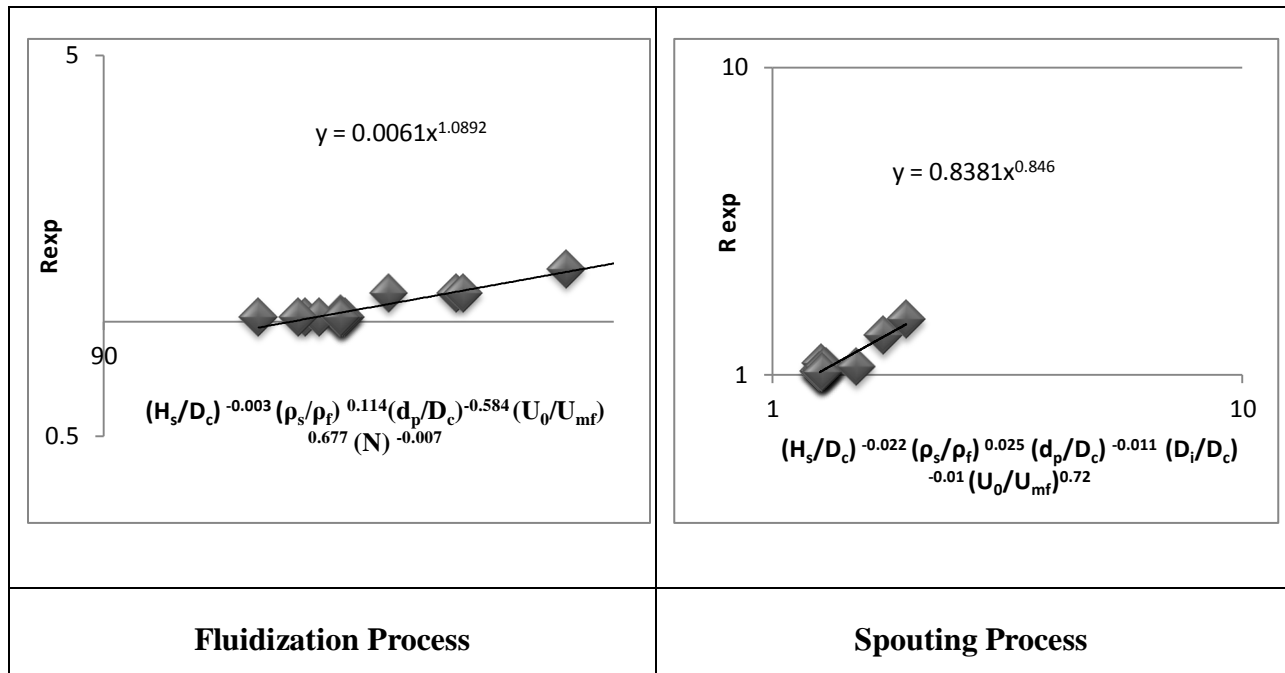
(a) Bed Pressure Drop

(b) Bed expansion ratio

(c) Bed Fluctuation ratio

(d) Fluidization Index
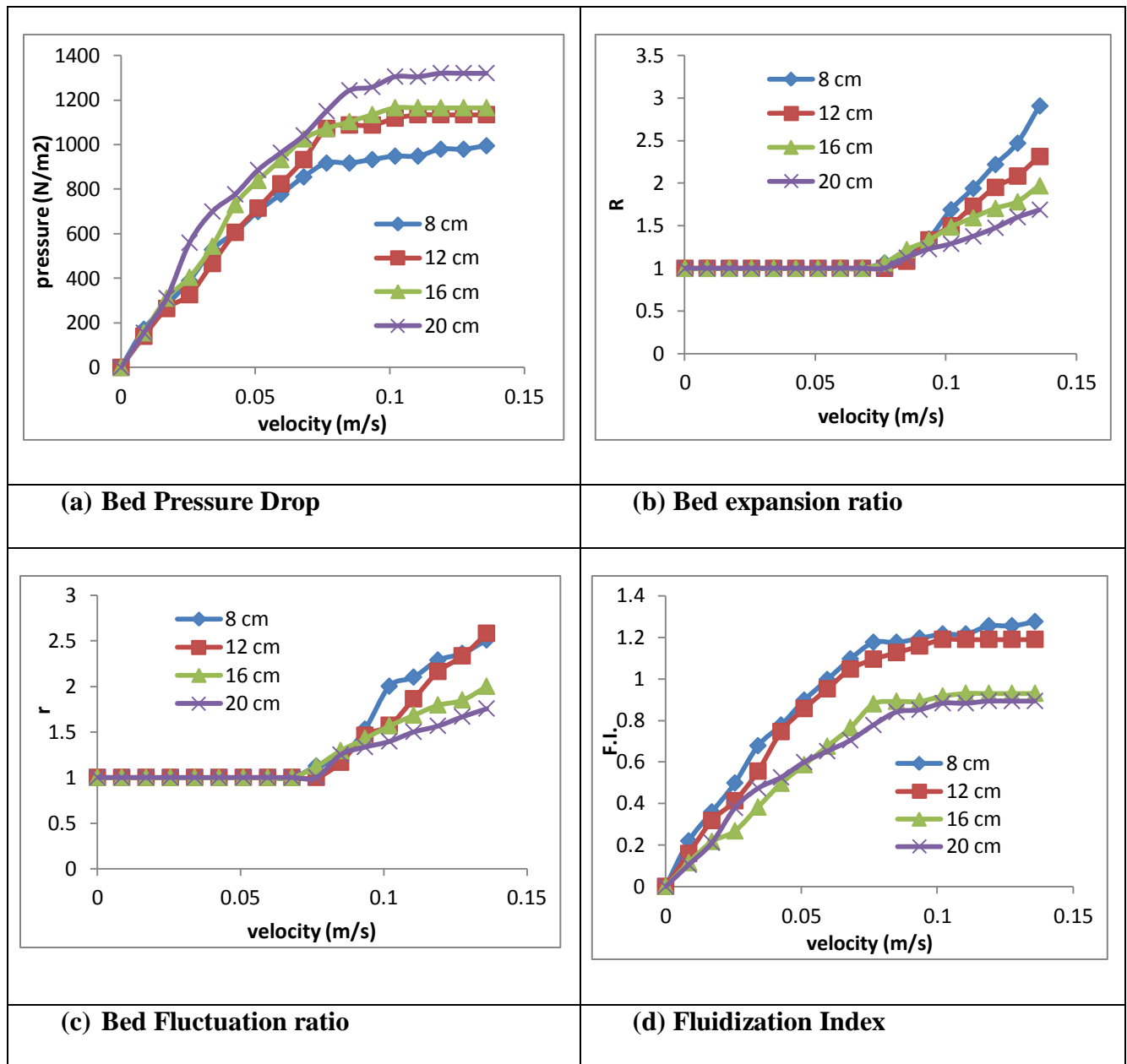
Figure - 6.7: Comparison of Variation in Bed Dynamics with Superficial Velocity of Fluid for Different Static Bed Heights for Nano Particles

(a)Bed Pressure Drops

(b)Bed Expansion ratio

(c)Bed Fluctuation Ratio

(d)   Fluidization Index

Figure - 6.8: Comparison of Variation in Bed dynamics with Superficial Velocity for Different Amounts of External force for Nano Particles

CHAPTER – 7

CONCLUSION

CONCLUSION

The hydrodynamic study of the fluidized / spouted bed has been carried out by calculating the bed expansion / fluctuation ratio and fluidization index of coarse (regular / irregular), fine and nano particles.

The bed expansion ratio and fluctuation ratio for the fluidized bed are observed to decrease with the increased speed of the stirrer (N) as the rotation of the stirrer prevents the bubble formation. The bed e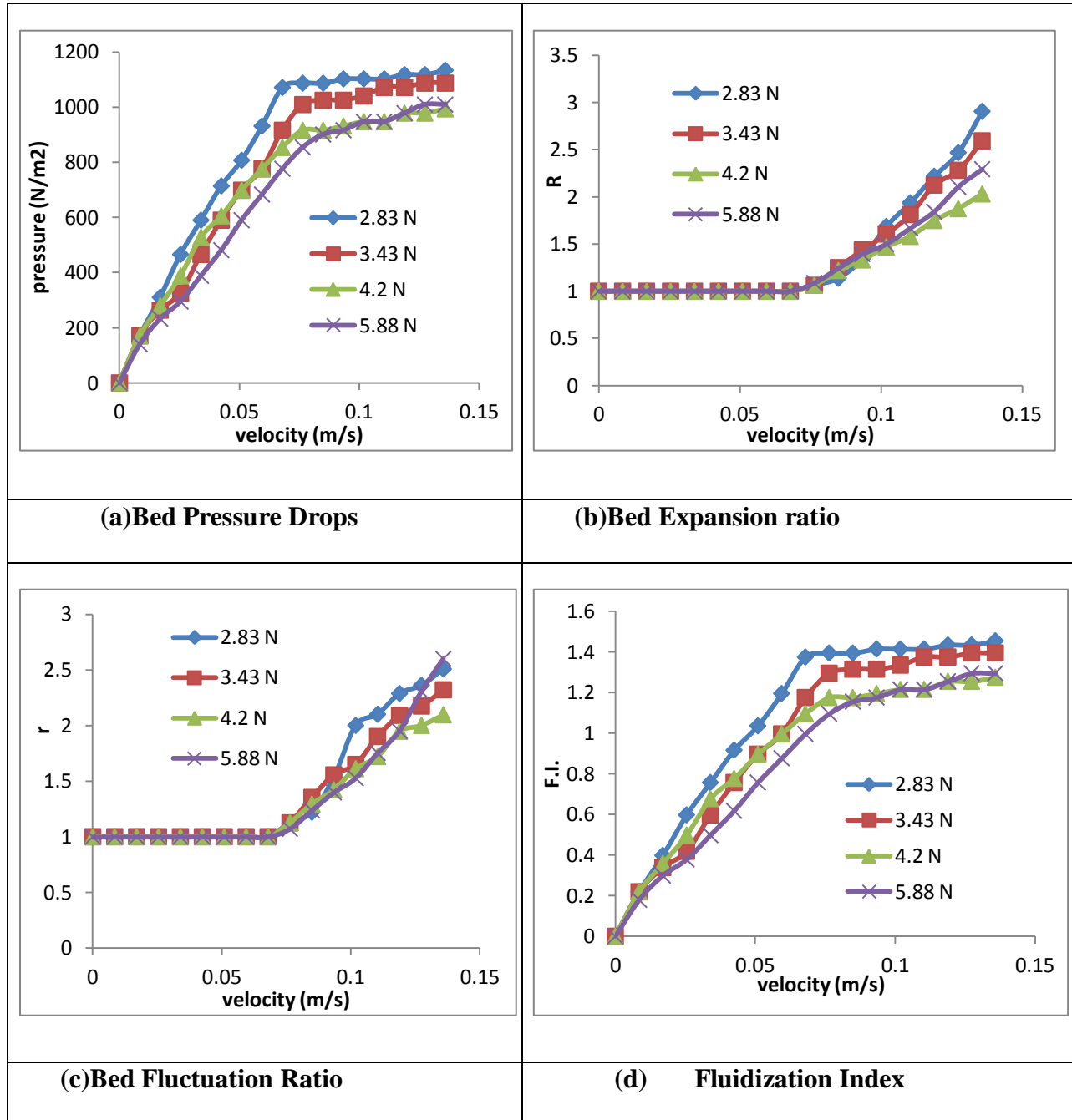xpansion ratios are observed to increase with the increased density of the particles but the variation of bed fluctuation ratio with the density of particles is observed to decrease for the fluidized bed.

With the view of satisfactory fluidization achieved by using a stirrer in the fluidized bed provides some agitation by which fine powders do not stick to the wall of the column thereby the formation of agglomerates is prevented. Thus uniform fluidization is achieved. Therefore the stirrer may also be used in fluidized bed reactor where catalysts are mainly smaller in size to provide large surface area for effective reactions to occur. This method can be applicable in any industry system i.e. drying of fine particles. This may also use in fluidized bed reactor where catalysts are mainly smaller in size to provide large surface area for reaction to occur and also gives the fundamentals optimum design of fluidized bed reactor.

The preliminary study has shown that fluidization of nano particle can be easily and smoothly fluidized with the assistance of external force. Thus it can be concluded that applying external force i.e. centrifugal force improves the bed dynamics to a great extent thereby minimizing the energy consumption. Therefore an external arrangement for creating some force

on outside of the column will be best option to improve the bed dynamics as well as economy of the process.

Correlations were developed for the bed expansion / fluctuation ratio and fluidization Index by varying different system parameters. The overall changes in values of bed expansion / fluctuation ratios, and fluidization Index were observed from the developed correlations. The calculated values of bed dynamics obtained through developed correlation or dimensional analysis are in good agreement with the experimentally observed values of bed dynamics. Comparing the calculated values of different bed dynamics obtained through developed correlations deviations are found to be within +15% to -15%. Thus the developed correlations can be used suitably over a wide range of system parameters for the study of bed behavior of fluidized bed as well as spouted bed reactor in industries over a wide range of parameters.

The knowledge of bed dynamics also gives the fundamentals for optimum design of fluidized bed reactor, gasifies and combustors, especially in the fixation of bed heights for such units. These models can be suitably scaled up for pilot plant units or for industrial uses. The developed correlations can also be used as the basis of designs for the industrial fluidized or spouted bed reactors, especially in Pharmaceutical industry. The developed correlation can further be used successfully for the calculation of bed dynamics such as bed expansion/fluctuation ratio and fluidization index with spherical / non spherical, coarse, fine and nano particles in chemical industries. Predication of bed expansion/ fluctuation ratios and fluidization index is of significance in gas- solid fluidization as their numerical values quantify the fluidization quality and in addition, the design fundamentals for gas-solid fluidization system.

The CFD simulation exhibited a solid circulation pattern for all the operating condition. The good agreement between the values obtained from CFD simulation and experimental ones with the present operating condition, it can be concluded that the Eulerian - Eulerian multi- phase granular flow approach is capable to predicting the overall performance of gas- solid fluidized bed. Thus the dynamic characteristics of gas – solid fluidization for fine particles obtained from CFD simulation validates with the experimental results, thereby the developed correlations are validated.

The calculated values of bed expansion ratio obtained through CFD simulation analysis have been compared with the experimentally observed values for the laboratory scale fluidized bed column. The comparison shows that the percentage deviation between calculated values of experimental and the values obtained through CFD simulation are very less.

7.1 SCOPE AND FUTURE WORK

- ❖ Hydrodynamic behaviors of nano particles to be studied by varying different system parameters.
- ❖ To develop correlation for the hydrodynamics behaviors of nano particles.
- ❖ Hydrodynamic behaviors of nano particles to be simulated by CFD Simulation.
- ❖ Validation of bed dynamics of nano particles with experimental and CFD simulation.

NOMENCLATURE

H	:	Bed height, cm
D	:	Diameter, cm
d	:	Particle diameter, microns
U	:	Velocity of air, m/s
N	:	Velocity of rod promoter, rpm
R	:	Expansion ratio
r	:	Fluctuation ratio
r	:	Radius of rubber tube, m
ΔP	:	Pressure drop, N/m^2
W	:	Weight of material, gm
A	:	Area of cross-section, cm^2
u	:	velocity in phase, m/s
F_i	:	Inter-phase momentum exchange
F	:	Force, N
F	:	Centrifugal Force, N
K	:	Interphase exchange coefficient, kg/s
C_D	:	drag coefficient
I	:	Identity matrix
σ	:	Coefficient in turbulent parameter
G	:	Generation of turbulence
S_k	:	User- defined source term
Π_{kg}	:	Dispersed phase in continuous gas phase

k_{jg}	:	Covariance velocity of continuous gas phase
u_{jg}	:	Relative velocity, m/s
u_{dr}	:	Drift velocity, m/s
C_1, C_2, C_3	:	Coefficient in turbulent parameter
m	:	Mass of bed materials, kg

Greek Symbols

ρ	:	density, gm/cc
ϵ	:	Volume fraction
ϵ	:	Dissipation rate, m^2/s^3
τ	:	Stress-strain tensors, Pa
μ	:	Viscosity, Pa s
λ	:	Bulk viscosity, Pa s
ω	:	Angular velocity, rpm

Subscripts

S	:	static
max	:	Maximum
min	:	Minimum
avg	:	Average
C	:	Column
i	:	Spout
o	:	Superficial
mf	:	Minimum fluidization / spout
p	:	Particle

k	:	Phase
k	:	Kinetic energy, J
f	:	Fluid
g	:	Gas
s	:	Solid
L	:	Lift
D	:	Drag
VM	:	Added mass
gs	:	Inter phase of gas and solid
t	:	Turbulent
j	:	No. of secondary phases

Superscripts

| T | : | Transpose |

Abbreviations

CFD	:	Computational fluid dynamics
cal	:	Calculated
exp	:	Experimental
F.I.	:	Fluidization Index
2D	:	Two dimensional
R_{ep}	:	Particles Reynolds's number
CVM	:	Constant viscosity model
KTGF	:	Kinetic theory granular flow
NAFB	:	Nano-agglomerate fluidized bed

BC : Boundary conditions

APF : Agglomerate particulate fluidization

ABF : Agglomerate bubbling fluidization

REFERENCES

- "ANSYS FLUENT 12.0", Theory Guide, 2009.

- "ANSYS FLUENT 12.0", User's Guide, 2009.

- Avidan A. A. and Yerushalmi J., "Bed expansion in high velocity fluidization", Powder Technology; 32, 223-232, 1982.

- Bacelos M. S. and Freire J. T., "Flow regimes in wet conical spouted beds using glass bead mixtures", Particuology; 6: 72–80, 2008.

- Bahramian A. R. and Mansour K., "CFD Modeling of TiO_2 nano-agglomerates hydrodynamics in a conical fluidized bed unit with experimental validation", Iran. J. Chem. Chem. Eng.; Vol. 29, No. 2, 2010.

- Cardoso C.R., Ataide C.H. and Abreu J.M. Minimum fluidization velocity of fine particle, Material science forum; 591: pp. 335-340, 2008.

- Cody G.D., Goldfarb D.J., Storch G.V., and Norris A.N., "Particle granular temperature in gas fluidized beds". Powder Technology; 87: 211–232, 1996.

- Goldschmidt M. J. V., Kuipers J. A. M. and Swaaij W. P. M., "Hydrodynamic modeling of dense gas-fluidized beds using the kinetic theory of granular flow: effect of coefficient of restitution on bed dynamics", Chemical Engineering Science; 56, 571-578, 2001.

- Hakim L. F., Portman J.L., Casper M.D. and Weimer A.W., "Aggregation behavior of nano particles in fluidized beds", Powder Technology; 160, 149 – 160, 2005.

- Hamzehei M., Rahimzadeh H. and Ahmadi G., "Studies of gas velocity and particles size effects on fluidized bed hydrodynamics with CFD modeling and experimental investigation", Journal of Mechanics; Vol. 26, No. 3, 2010.

- Huang C.,Wang Y. and Wei F., "Solids mixing behavior in a nano-agglomerate fluidized bed", Powder Technology; 182, 334–341, 2008.

- Jaraiz E., Kimura S. and Levenspiel O., "Vibrating beds of fine particles: estimation of inter particle forces from expansion and pressure drop experiments", Powder Technology; 72, 23-30, 1992.

- Jung J. and Gidaspow D., "Fluidization of nano-size particles", Journal of Nano particle Research; 4: 483–497, 2002.

- Kumar A. and Roy G.K., "Bed dynamics of gas-solid fluidized bed with rod promoter", China particulogy; 5, pp. 261-266, 2007.

- Kunii D. and Levenspiel O., "Fluidization Engineering", Second Ed., Butterworth-Heinemann, Boston, 1991.

- Kusakabe K., Kuriyama T. and Morooka S., "Fluidization of fine particles at reduced pressure", Powder Technology; 58, 125 – 130, 1989.

- Laszuk A., Pabisand M., Berengarten G., "Fluidization of fine materials", Chemical and Petroleum Engineering; Vol. 44, Nos. 9–10, 2008.

- Mathur K.B. and Epstein N., "Spouted Beds", Academic Press, New York, 1974.

- Mawatari Y., Tsunekawa M., Tatemoto Y. and Noda K., "Favorable vibrated fluidization conditions for cohesive fine particles", Powder Technology; 154, 54 – 60, 2005.

- Nam C.H., Pfeffer R.,Dave R. N. and Sundaresan S., "Aerated vibro fluidization of silica nano particles", Journal of American Institute of Chemical Engineers; 50: 1776–1785, 2004.

- Olazar M., San Jose M. J., Lamosas R. L. and Bilbao J., "Hydrodynamics of sawdust and mixtures of wood residues in conical spouted beds", Ind. Eng. Chem. Res., 33, 993-1000, 1994.

- Olazar M.,San Jose M. J., Pefias F. J. and Bilbao J. "Stability and hydrodynamics of conical spouted beds with binary mixtures" Ind. Eng. Chem. Res.; 32, 2826-2834, 1993.

- Olazar M.,San Jose M.J., Aguayo A.T., Arandes J.M. and Bilbao J., "Hydrodynamics of nearly flat base spouted beds", The Chemical Engineering Journal; 55, 27-37,1994.

- Padhi S. K. and Singh R.K., "Hydrodynamics studies of gas- solid fluidization in hexagonal bed for non-spherical particles", Journal of scientific and industrial Research; volume 68: pp. 951- 954, 2009.

- Rooney N.M. and Harrison D. "Spouted beds of fine particles", Powder Technology; 9 227-230,1974.

- Russo P., Chirone R., Massimilla L. and Russo S., "The influence of the frequency of acoustic waves on sound-assisted fluidization of beds of fine particles", Powder Technology; 82, 219-230,1995.

- Sahoo A., "Bed expansion and fluctuation in cylindrical gas -solid fluidized beds with stirred promoters", Advanced Powder Technology Journal; 22,753-760, 2011.

- Sau D.C. and Biswal K.C., "Computational fluid dynamics and experimental study of the hydrodynamics of a gas–solid tapered fluidized bed", Applied mathematical modeling; 35, 2265 -2278, 2011.

- Sau D.C., Mohanty S. and Biswal K.C., "Experimental studies and empirical models for the prediction of bed expansion in gas–solid tapered fluidized beds", Chemical engineering and processing; 49, 418–424, 2010.

- Shan J.,Guobin C., Fan M., Yu B., Wang J. and Yong J., "Fluidization of fine particles in conical beds", Powder Technology; 118, 271–274,2001.

- Singh R.K. and Roy G.K., "Prediction of fluctuation ratio for gas–solid fluidization in cylindrical and non-cylindrical beds", Indian journal of chemical technology; volume 13 pp. 139 -143, 2006.

- Singh R.K. and Roy G.K., "Prediction of minimum bubbling velocity, fluidization index and range of particulate fluidization for gas–solid fluidization in cylindrical and non-cylindrical beds", Powder Technology; 159, 168 – 172, 2005.

- Taghipour F., Ellis N. and Wong C., "Experimental and computational study of gas–solid fluidized bed hydrodynamics", Chemical Engineering Science; 60, 6857 – 6867, 2005.

- Valverde J.M., Espin M.J., Quintanilla M.A.S. and Castellanos A., "Magneto fluidization of fine magnetite powder", Physical Review 79, 031306, 2009.

- Wang X.S., Rahman F. and Rhodes M.J., "Nano particle fluidization and Geldart's classification", Chemical Engineering Science; 62, 3455 – 3461, 2007.

- Wang Z., Kwauk M. and Li H., "Fluidization of fine particles", Elsevier Science Ltd PII: S0009-2509, 00280-7, 1997.

- Xu C. and Zhu J., "Parametric study of fine particle fluidization under mechanical vibration", Powder Technology; 161, 135 – 144, 2006.

- Zhiping Z., Yongjie N. and Qing gang L., "Effect of pressure on minimum fluidization Velocity", Journal of thermal science; Vol.16, No.3, 264—269, 2007.

- Zhong W.,Zhang M.,Jin B., "Maximum spoutable bed height of spout-fluid bed", Chemical Engineering Journal; 124; 55–62,2006.

- Zhu C., Yu Q., DaveR. N. and Pfeffer R., "Gas fluidization characteristics of nanoparticle agglomerates"; 51: 426–439, 2005.